ハンチントン病原因遺伝子産物huntingtinの細胞内凝集体形成が促進される可能性も示唆されている[14]．すなわち，成熟神経回路における正常な神経細胞骨格の役割の一つは，タンパク質の流通・品質管理を通じて，異常なタンパク凝集体形成を未然に防ぐことであるといえる．このことに合致して，前述したRhoGAP分子oligophrenin-1変異の研究から，Rhoシグナリングが破綻すると，シナプス前ならびにシナプス後機能の両者において，小胞輸送やレセプタートラフィッキングに顕著な異常が現れることが判明している[15)~17)]．すなわち，低分子量Gタンパク質を介したアクチン細胞骨格動態制御によって，成熟神経回路のシナプス伝達・シナプス可塑性の発現が刻一刻と決定されている可能性が強く示唆されている．

5．神経疾患における細胞骨格動態への薬理学的介入による機能回復の試み

このように，細胞骨格系の機能破綻により，多くの脳高次機能異常，さらには神経・精神疾患の発症が引き起こされる可能性が高い．では，このような細胞骨格動態の異常を薬理学的に回復する戦略は不可能なのであろうか．いったん発達期に起きてしまった回路形成異常を元に回復することは困難であることが予測されるが，成体脳における情報伝達異常については，薬理学的回復の可能性がある．もしそうであれば，これにより，病態が果たしてどのように改善するか，大いに期待される．

実際，アルツハイマー病のアミロイド沈着やポリグルタミン凝集体の形成がROCK阻害薬により改善するという報告が数年前から発表されてきている[14]．また，現時点ではあくまでも遺伝子改変マウスレベルでの知見に留まっているが，oligophrenin欠損マウスにおけるRhoシグナル活性化に伴うシナプス伝達・可塑性異常は，成体でもRhoシグナル伝達系の抑制により回復することが明らかとなっている[17]．このように，いまだ断片的な実験事実によってしか支持されていないが，細胞骨格制御破綻によってもたらされる神経疾患の少なくとも一部については，ROCK阻害薬などの薬剤の効果の検証が待たれるところである．

一方，神経回路網形成の初期には，神経細胞におけるRho/ROCK/mDia1シグナル伝達系が突起形成・伸展の制御に関与している[18]．このことは，脊髄損傷などによる後天的な突起発達障害のケースにおいて，Rhoシグナルの人為的修飾により，神経突起再生を誘導・制御するという新たなアプローチの可能性を示唆するものである．事実，そのような試みはすでに米国・カナダでは実際に始まりつつある．McKerracherらは，MAGやNogo-66など神経損傷後の軸索再生を抑制する諸因子がp75NGFRを介して，脊髄損傷後に脊髄における低分子量GタンパクRho活性が持続的に上昇することを見出した．そしてマウス胸髄損傷モデルを用い，脊髄切断後早期にRho活性やROCK活性を遮断することにより，軸索再生スピードの有意な加速や，運動能の著しい回復を得ることに成功している[19]．ラット胸髄切断モデルを用いたStrittmatterらも，ROCKインヒビター投与時には，同様に神経線維再生・運動能回復がともに促進されることを追認していることは特筆に値する[20]．

これらの報告から大胆に考察してみると，Rho/ROCK情報伝達系は，ほかの低分子量Gタンパク質経路と協調的あるいは拮抗的に連携しながら，アクチン細胞骨格制御を介し，単に形態制御をおこなうのみでなく，神経細胞内の種々のタンパクの輸送・集積・品質管理・分解に対しても何らかの恒常的制御を及ぼしているのかも知れない（図　）．このような観点からもROCKインヒビターの神経疾患に対する創薬標的としての新たな可能性について，今後検証することが急務と考えられる．

おわりに

発育時における脳神経回路網の発達異常が，精神・認知・神経の障害をもたらす原因の一つであるという考え方が最近有力視されている．またいったん正常な発育を遂げた場合でも，正常範囲の加齢とともに，脳神経回路網の機能的異常が蓄積し，脳高次機能（意識，情動，記憶，意欲，注意など）の機能障害が高い確率で襲ってくるといわれている．今日までに得られた知見により，脳神経系における細胞骨格制御が新たな分子治療のための創薬標的となりつつあり，神経回路網損傷や神経変性による脳高次機能低下から回復する，という可能性が実現可能なレベルまで徐々に到達しつつあることを，本稿で

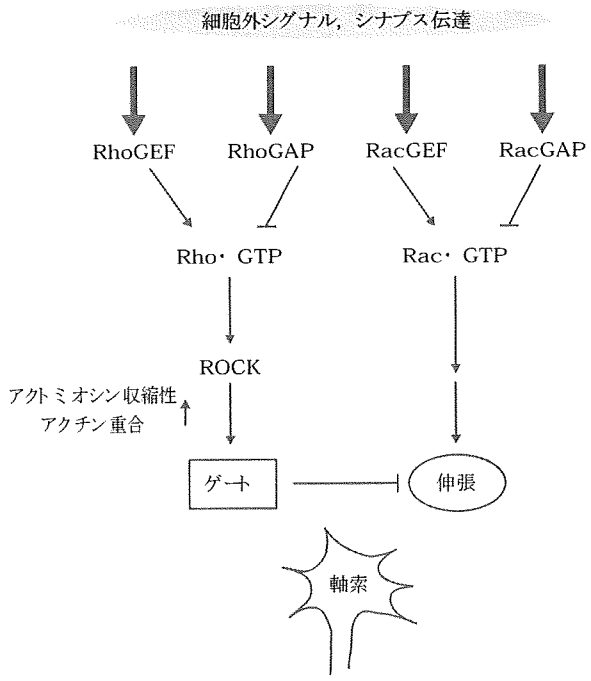

図　神経細胞骨格の作用点に対する2重制御の原理：突起伸張の例 筆者作成）
突起伸張 axon growth）に対しては，2つの低分子量Gタンパク Rac と Rho が拮抗的に2重制御をかけているため，たとえば Rac による正の制御の低下を，Rho による負の制御の抑制により代償することが可能となる．ROCK 阻害薬は，Rho 下流の多くの ROCK 作用点に対して効果をもつ．小胞輸送，レセプタートラフィッキングにおいても同様の2重制御機構の存在が想定されているがその分子的実体はまだ不明である．

は紹介した．今後の神経細胞骨格シグナル伝達の理解が深まれば，精神遅滞や精神疾患の動物モデルにおいても，シナプス形成・維持やスパイン形態の操作・修復までが制御可能となると信じ，期待して止まない次第である．

文　献

1) Cajal SR: *Textura del sistema nervioso del hombre y de los vertebrados* (Textbook on the nervous system of man and the vertebrates), 2002, pp.1897–1899
2) Principles of Neural Science, Fourth Edition. ed by Kandel ER *et al*, McGraw–Hill, New York, 2000
3) Hebb DO: The Organization of Behavior: A Neuropsychological Theory, Wiley 1949.
4) Matsuzaki M *et al*: Structural basis of long–term potentiation in single dendritic spines. *Nature* 429: 761–766, 2004
5) Kuriu T *et al*: Differential control of postsynaptic density scaffolds via actin–dependent and–independent mechanisms. *J Neurosci* 26: 7693–7706, 2006
6) Nonaka M *et al*: Essential contribution of the ligand–binding beta B/beta C loop of PDZ1 and PDZ2 in the regulation of postsynaptic clustering, scaffolding, and localization of postsynaptic density–95. *J Neurosci* 26: 763–774, 2006
7) Olson EC *et al*: Smooth, rough and upside–down neocortical development. *Curr Opin Genet Dev* 12: 320–327, 2002
8) Chechlacz M *et al*: Is mental retardation a defect of synapse structure and function? *Pediatr Neurol* 29: 11–17, 2003
9) Khelfaoui M *et al*: Loss of X–linked mental retardation gene oligophrenin 1 in mice impairs spatial memory and leads to ventricular enlargement and dendritic

spine immaturity. *J Neurosci* 27: 9439–9450, 2007
10) Hayashi ML *et al*: Altered cortical synaptic morphology and impaired memory consolidation in forebrain-pecific dominant-negative PAK transgenic mice. *Neuron* 42: 773–787, 2004
11) Lynch ED *et al*: Nonsyndromic deafness DFNA1 associated with mutation of a human homolog of the Drosophila gene diaphanous. *Science* 278: 1315–1318, 1997
12) Meng Y *et al*: Abnormal spine morphology and enhanced LTP in LIMK-1 knockout mice. *Neuron* 35: 121–133, 2002
13) Heredia L *et al*: Phosphorylation of actin-depolymerizing factor/cofilin by LIM-kinase mediates amyloid beta-induced degeneration: a potential mechanism of neuronal dystrophy in Alzheimer's disease. *J Neurosci* 26: 6533–6542, 2006
14) Shao J *et al*: Phosphorylation of profilin by ROCK1 regulates polyglutamine aggregation. *Mol Cell Biol* 28: 5196–5208, 2008
15) Nakano-Kobayashi A et al: The Rho-linked mental retardation protein OPHN1 controls synaptic vesicle endocytosis via endophilin A1. *Curr Biol* 19: 1–7, 2009
16) Kasri NN *et al*: The Rho-linked mental retardation protein oligpphrenin-1 controls synapse maturation and plasticity by stabilizing AMPA receptors. *Genes Dev* 23: 1289–1302, 2009
17) Khelfaoui M *et al*: Inhibition of RhoA pathway rescues the endocytosis defects in oligophrenin1 mouse model of mental retardation. *Hum Mol Genet* 18: 2575–2583, 2009
18) Bito H: Dynamic control of neuronal morphogenesis by rho signaling. *J Biochem* 134: 315–319, 2003
19) Dergham P *et al*: Rho signaling pathway targeted to promote spinal cord repair. *J Neurosci* 22: 6570–6577, 2002
20) Fournier AE *et al*: Rho kinase inhibition enhances axonal regeneration in the injured CNS. *J Neurosci* 23: 1416–1423, 2003

BITO Haruhiko

びとう・はるひこ
1990年，東京大学医学部卒業
1993年，同大学院修了(博士)医学，授与)
1993～97年，スタンフォード大学大学院医学研究科常勤研究員
1997年，京都大学大学院医学研究科助手
1998年，同講師
2003年，東京大学大学院医学系研究科助教授
2007年，同准教授 現職)
専門は，神経生化学
趣味は，読書，音楽鑑賞

TAKEMOTO-KIMURA Sayaka

たけもと-きむら・さやか
1999年，名古屋大学医学部卒業
1999年，同大学医学部付属病院医員 研修医)
2000～03年，京都大学大学院医学研究科大学院生
2003年，同大学院博士課程修了 京都大学博士 医学)学位取得)
2003年，東京大学大学院医学系研究科神経生化学助手
2007年，同助教 現職)
専門は，神経生化学，とくに神経回路形成と可塑性の分子機構
趣味は，子供との東大散策

Acta Crystallographica Section F
Structural Biology and Crystallization Communications
ISSN 1744-3091
Editors: H. M. Einspahr and M. S. Weiss

Crystallization of mitochondrial rhodoquinol-fumarate reductase from the parasitic nematode *Ascaris suum* with the specific inhibitor flutolanil

Arihiro Osanai, Shigeharu Harada, Kimitoshi Sakamoto, Hironari Shimizu, Daniel Ken Inaoka and Kiyoshi Kita

Acta Cryst. (2009). F**65**, 941–944

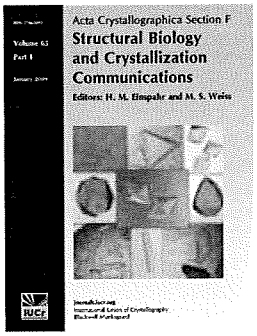

Acta Crystallographica Section F
Structural Biology and Crystallization Communications
ISSN 1744-3091

Crystallization of mitochondrial rhodoquinol-fumarate reductase from the parasitic nematode *Ascaris suum* with the specific inhibitor flutolanil

Arihiro Osanai,[a] Shigeharu Harada,[b] Kimitoshi Sakamoto,[a]* Hironari Shimizu,[a] Daniel Ken Inaoka[a] and Kiyoshi Kita[a]

[a]Department of Biomedical Chemistry, Graduate School of Medicine, University of Tokyo, 7-3-1 Hongo, Bunkyo-ku, Tokyo 113-0033, Japan, and [b]Department of Applied Biology, Graduate School of Science and Technology, Kyoto Institute of Technology, Sakyo-ku, Kyoto 606-8585, Japan

Correspondence e-mail: sakamok@m.u-tokyo.ac.jp

Received 2 June 2009
Accepted 8 August 2009

In adult *Ascaris suum* (roundworm) mitochondrial membrane-bound complex II acts as a rhodoquinol-fumarate reductase, which is the reverse reaction to that of mammalian complex II (succinate-ubiquinone reductase). The adult *A. suum* rhodoquinol-fumarate reductase was crystallized in the presence of octaethyleneglycol monododecyl ether and *n*-dodecyl-β-D-maltopyranoside in a 3:2 weight ratio. The crystals belonged to the orthorhombic space group $P2_12_12_1$, with unit-cell parameters $a = 123.75$, $b = 129.08$, $c = 221.12$ Å, and diffracted to 2.8 Å resolution using synchrotron radiation. The presence of two molecules in the asymmetric unit (120 kDa × 2) gives a crystal volume per protein mass (V_M) of 3.6 Å^3 Da^{-1}.

1. Introduction

In parasites, fumarate plays an important role in redox homeostasis. The parasitic protozoan *Trypanosoma cruzi* utilizes bacterial-type dihydroorotate dehydrogenase (TcDHOD), which is the fourth enzyme in the pyrimidine-biosynthesis pathway and catalyzes the oxidation of dihydroorotate and the reduction of fumarate to succinate. We have elucidated the catalytic mechanisms of these sequential reactions by determination of the three-dimensional structures of TcDHOD in the ligand-free form and in complex with the substrates (dihydroorotate and fumarate), product (orotate and succinate) and inhibitor (oxonate) at atomic resolution (Inaoka *et al.*, 2008).

In parasitic helminths, fumarate is the terminal electron acceptor of the anaerobic respiratory chain, which is essential for the survival of the parasites in the host (Kita & Takamiya, 2002). Complex II catalyzes fumarate reduction in anaerobic respiration and functions as a terminal oxidase. In eukaryotes, complex II (succinate-ubiquinone reductase in aerobic respiration; SQR) is located in the inner mitochondrial membrane and is generally composed of four polypeptides. The flavoprotein (Fp) subunit is the largest, with an approximate molecular mass of 70 kDa, and contains flavin adenine dinucleotide (FAD) as a prosthetic group. Complex II contains a relatively hydrophilic catalytic region formed by the Fp subunit and an iron–sulfur cluster (Ip) subunit, which has a molecular mass of approximately 30 kDa. The remaining subunits comprise cytochrome *b*, which contains a haem *b*. Cytochrome *b* is composed of two hydrophobic membrane-anchoring polypeptide subunits, namely a 15 kDa large subunit (CybL) and a 13 kDa small subunit (CybS). These cytochrome *b* subunits are necessary for the interaction of complex II with hydrophobic membrane-associated quinones such as ubiquinone (UQ) and rhodoquinone (RQ).

Our recent study on the respiratory chain of the parasitic nematode *Ascaris suum* has shown that the mitochondrial NADH-fumarate reductase system plays an important role in the anaerobic energy metabolism of adult parasites inhabiting hosts and that they undergo unique developmental changes during their life cycle (Kita & Takamiya, 2002; Iwata *et al.*, 2008). In anaerobic metabolism by *A. suum* mitochondria, the transfer of a reducing equivalent from NADH to the low-potential RQ is conducted by the NADH–RQ reductase complex (complex I). This pathway ends with the production of succinate by the rhodoquinol-fumarate reductase (QFR) activity of complex II. Electron transfer from NADH to fumarate is

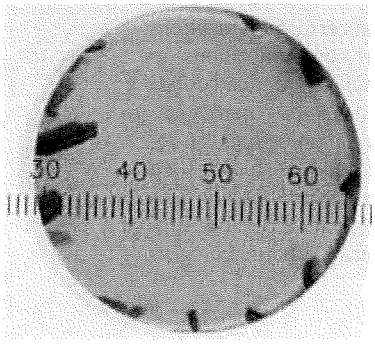

coupled to site I phosphorylation of complex I *via* the generation of a proton gradient. The difference in redox potential between the NAD^+/NADH couple (E'_m = −320 mV) and the fumarate/succinate couple (E'_m = +30 mV) is sufficient to drive ATP synthesis.

The anaerobic NADH-fumarate reductase system is found not only in nematodes but also in bacteria and many other parasites and is a promising target for chemotherapy (Omura *et al.*, 2001; Tielens *et al.*, 2002; Matsumoto *et al.*, 2008). The most potent inhibitor of complex II, atpenin A5, was found during screening for inhibitors of *A. suum* complex II (Miyadera *et al.*, 2003). However, the mammalian complex II is much more sensitive to atpenin A5 than the *A. suum* enzyme. By further screening, we have found that flutolanil, a commercially available fungicide (Ito *et al.*, 2004), specifically inhibits the *A. suum* complex II. Therefore, we have taken flutolanil as a lead compound for structure-based drug design. In the current study, we have purified, crystallized and performed preliminary X-ray diffraction studies on the adult *A. suum* QFR.

2. Methods

2.1. Purification

Mitochondria were prepared from the muscle of adult *A. suum* as described by Takamiya *et al.* (1984), except that Chappell–Perry medium (100 m*M* KCl, 50 m*M* Tris–HCl pH 7.4, 1 m*M* ATP, 5 m*M* $MgSO_4$ and 1 m*M* EDTA; Ernster & Nordenbrand, 1967) was used instead of MSE medium (210 m*M* mannitol, 70 m*M* sucrose and 0.1 m*M* EDTA). The QFR was solubilized from adult *A. suum* mitochondria in 1.0%(*w*/*v*) sucrose monolaurate (Dojindo) and purified in the presence of 0.1%(*w*/*v*) sucrose monolaurate. *A. suum* mitochondria (1 g protein) were homogenized in 500 ml buffer *A* (10 m*M* Tris–HCl pH 7.5, 1 m*M* sodium malonate) containing 1.0%(*w*/*v*) sucrose monolaurate. After incubating the mixture for 30 min at 277 K, it was centrifuged for 1 h at 200 000*g*. The clear reddish-brown supernatant containing the solubilized QFR was applied onto a GE Healthcare DEAE Sepharose FF column (2.6 × 24 cm) pre-equilibrated with buffer *A* containing 0.1%(*w*/*v*) sucrose monolaurate. After washing the column with the same buffer, the QFR was eluted with 2400 ml of the buffer containing a linear gradient of 0.0–0.3 *M* NaCl. Fractions containing the QFR, which started to elute at approximately 0.1 *M* NaCl, were pooled and adjusted to 0.15 g ml^{-1} polyethylene glycol 3350 (Hampton Research) to precipitate the QFR. The mixture was centrifuged for 20 min at 15 000*g* and the precipitate was dissolved in buffer *A* containing 0.1%(*w*/*v*) sucrose monolaurate. The QFR was then further loaded onto a GE Healthcare Source 15Q column (1.6 × 10 cm) and eluted with 400 ml of buffer containing a linear gradient of 0–0.3 *M* NaCl. Fractions containing pure QFR as judged by SDS–PAGE (Fig. 1) were pooled. The purified QFR was then precipitated by adding solid polyethylene glycol (PEG) 3350 to 0.15 g ml^{-1} and stored at 193 K.

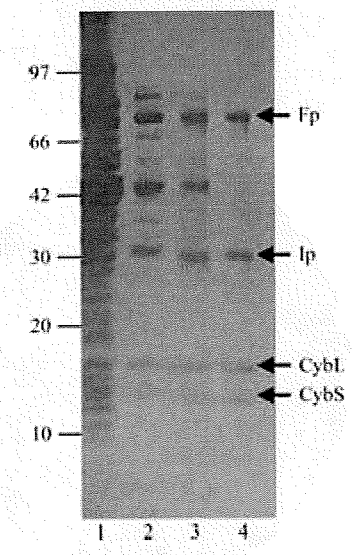

Figure 1
Purity of *A. suum* QFR at different stages of purification. Samples were separated by SDS–PAGE and the gel was stained with Coomassie Blue. The positions of molecular-weight markers are indicated on the left (in kDa) and the four subunits of *A. suum* QFR (Fp, flavoprotein subunit; Ip, iron–sulfur cluster subunit; CybL, cytochrome *b* large subunit; CybS, cytochrome *b* small subunit) are labelled on the right. Lane 1, whole mitochondria; lane 2, supernatant obtained after ultracentrifugation of the detergent extract; lane 3, pooled fractions from the DEAE Sepharose FF column; lane 4, pooled fractions from the Source 15Q column.

2.2. Crystallization

Conditions for crystallizing the *A. suum* QFR were screened using Crystal Screen (Jancarik & Kim, 1991) and Crystal Screen II (Hampton Research). Crystallization by hanging-drop vapour diffusion was carried out using 96-well CrystalClear Strips (Hampton Research). A droplet containing equal volumes of approximately 20 mg ml^{-1} QFR in buffer *A* containing detergent and reservoir solution was equilibrated against 100 µl reservoir solution.

Aggregates of microcrystals were observed at 293 K from reservoir solutions containing polyethylene glycols with medium molecular weights and 200 m*M* salts when octaethyleneglycol monododecyl ether (C12E8) was used as a detergent. Attempts to optimize the conditions by altering the PEG type (3350, 4000 and 6000), PEG concentration and pH and by using Additive Screen kits (Hampton Research) did not succeed in improving the crystallization. We therefore examined the effect of adding another detergent as an additive. 0.1 volume of detergent solution was added to a droplet of approximately 20 mg ml^{-1} QFR in buffer *A* containing 0.5%(*w*/*v*) C12E8 and an equal volume of reservoir solution and crystallization by hanging-drop vapour diffusion was carried out. After several days, small crystals (~10 µm; Fig. 2*a*) appeared at 293 K in drops from reservoir solutions composed of 14–18%(*w*/*v*) PEG 3350, 100 m*M* Tris–HCl pH 7.5–8.6, 200 m*M* NaCl and 1 m*M* sodium malonate when the drops included 0.3–0.5%(*w*/*v*) *n*-dodecyl-β-D-maltopyranoside (C12M). To determine the optimal ratio of C12E8 to C12M, crystallization was carried out using QFR dissolved in buffer *A* containing different concentrations of C12E8 and C12M. The best condition for crystallization (Fig. 2*b*) was achieved at a 3:2 C12E8:C12M weight ratio.

Crystals larger than 100 µm in size were grown by the microdialysis method as follows. The precipitate of the purified QFR stored at 193 K was dissolved in buffer *A* (approximately 10 mg ml^{-1}) containing 0.6%(*w*/*v*) C12E8, 0.4%(*w*/*v*) C12M and 200 m*M* NaCl. After incubation for 20 min on ice, the QFR was precipitated by adding an equal volume of 40%(*w*/*v*) PEG 3350. The precipitate obtained by centrifugation was dissolved in the same buffer, incubated for 20 min on ice and mixed with an equal volume of 40%(*w*/*v*) PEG 3350 to precipitate the QFR. This procedure was repeated several times in order to replace sucrose monolaurate with the added detergent. The precipitate was finally dissolved in buffer *A* containing 0.06%(*w*/*v*) C12E8, 0.04%(*w*/*v*) C12M and 0.2 *M* NaCl, giving an approximately 40 mg ml^{-1} QFR solution. After adding an equal volume of 23%(*w*/*v*) PEG 3350 to the QFR solution, undissolved materials were removed by centrifugation for 20 min at 20 000*g*. The supernatant was then sealed in a 5 µl microdialysis button and dialyzed against

reservoir solution containing 15.0%(*w*/*v*) PEG 3350, 100 m*M* Tris–HCl pH 8.4, 200 m*M* NaCl, 1 m*M* sodium malonate, 0.06%(*w*/*v*) C12E8 and 0.04%(*w*/*v*) C12M. Dark red plate-shaped crystals appeared within 24 h and grew to 100–200 µm after 2–3 d at 293 K (Fig. 2*c*).

X-ray diffraction data were collected on BL44XU at SPring-8 (Harima, Japan) and on BL-5A and NW12A at the Photon Factory (Tsukuba, Japan) by the rotation method. For X-ray diffraction experiments at 100 K, a QFR crystal mounted on a nylon loop was transferred successively to reservoir solution supplemented with 3.75, 7.5, 11.25 and 15% glycerol and was then frozen by rapid submergence in liquid nitrogen. Data were processed and scaled using *HKL*-2000 and *SCALEPACK* (Otwinowski & Minor, 1997).

3. Results and discussion

To obtain sufficient *A. suum* mitochondria for purification of the QFR, we slightly modified the standard protocol. Specifically, we used Chappell–Perry medium (Ernster & Nordenbrand, 1967) in place of the standard medium. This resulted in 0.95 mg mitochondria per gram of muscle and 0.3 µmol min^{-1} mg^{-1} mitochondrial succinate dehydrogenase activity, which represents a threefold increase in recovery and a fourfold increase in specific activity compared with the previous method (Takamiya *et al.*, 1984). Using this method, we obtained 7.5 mg pure enzyme (Fig. 1, lane 4) from 1 kg of adult *A. suum* muscle.

Because the success of membrane-protein crystallization strongly depends on which detergent is used, we tested a variety of commercially available nonionic detergents in the screening of crystallization conditions for the *A. suum* QFR. Aggregates of microcrystals were obtained under several crystallization conditions using the detergent C12E8, but we were unable to optimize the conditions. Instead, the optimal condition for producing crystals suitable for X-ray structure analysis was achieved when the sucrose monolaurate was exchanged for a 3:2 weight ratio of C12E8:C12M (Fig. 2*c*). Crystals grew to larger than 100 µm in 2–3 d by dialyzing QFR, which was dissolved in buffer *A* containing 11.5%(*w*/*v*) PEG 3350, 0.06%(*w*/*v*) C12E8, 0.04%(*w*/*v*) C12M and 200 m*M* NaCl, against reservoir solution containing 15.0%(*w*/*v*) PEG 3350, 100 m*M* Tris–HCl pH 8.4, 200 m*M* NaCl, 1 m*M* sodium malonate, 0.06%(*w*/*v*) C12E8 and 0.04%(*w*/*v*) C12M. Adding 11.5%(*w*/*v*) PEG 3350 to the QFR solution in advance prevented serious bubble formation in the microdialysis button, which was unfavourable for crystallization.

X-ray diffraction patterns were recorded from a single crystal at 100 K with an oscillation angle of 1.0° using a Bruker DIP-6040 imaging-plate detector on the BL44XU beamline at SPring-8. Analysis of the symmetry and the systematic absences in the recorded diffraction pattern indicated that the crystals belonged to the orthorhombic space group $P2_12_12_1$, with unit-cell parameters a = 123.75, b = 129.08, c = 221.12 Å. Assuming the presence of two QFR molecules (120 kDa × 2) in the asymmetric unit, the calculated Matthews coefficient V_M (Matthews, 1968) was 3.6 $Å^3$ Da^{-1}. A total of 587 189 observed reflections recorded on 180 images were merged to 75 372 unique reflections from 50.0 to 2.8 Å resolution.

During the screening of inhibitors, we found that flutolanil (Ito *et al.*, 2004), a commercially available fungicide, specifically inhibits *A. suum* SQR. The IC_{50} of flutolanil against *A. suum* and bovine SQR was 0.081 and 16 µ*M*, respectively, indicating that flutolanil is a promising lead compound for anthelminthics. To enable rational drug optimization, we prepared crystals of the *A. suum* QFR complexed with flutolanil by the soaking method. X-ray diffraction patterns were recorded at 100 K on 130 frames with an oscillation angle of 1° using an ADSC Quantum 315 CCD detector on NW12 at Photon Factory. A total of 54 964 unique reflections from 50.0 to 3.2 Å resolution were obtained. The data-collection and processing statistics are summarized in Table 1.

We attempted to solve the structure of the *A. suum* QFR by the molecular-replacement method using the *MOLREP* program (Navaza, 1994) as implemented within *CCP*4 (Collaborative Computational Project, Number 4, 1994) and the refined coordinates

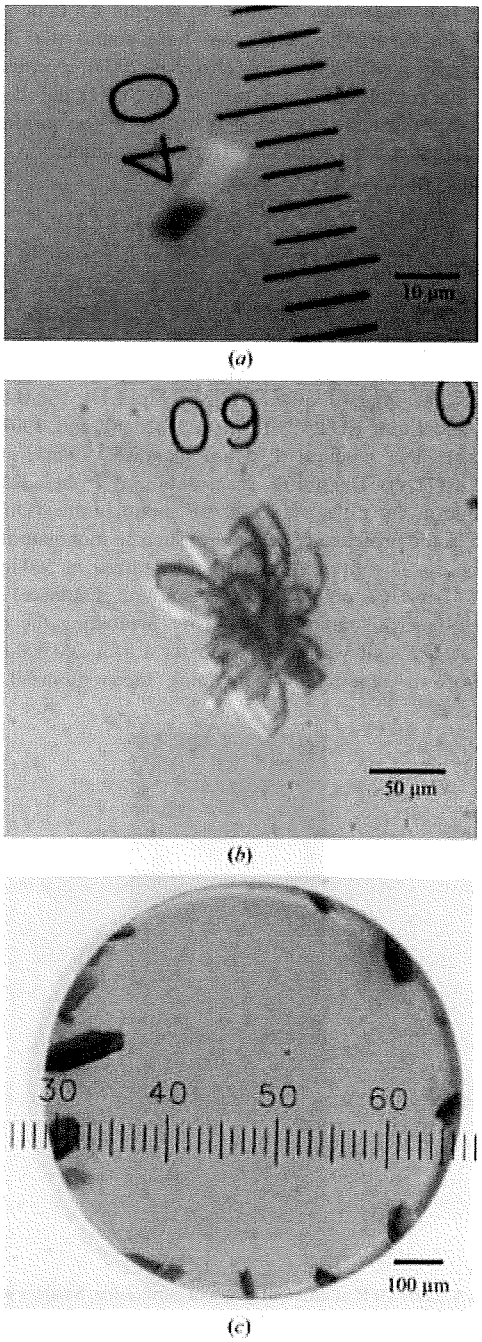

Figure 2
Typical crystals of *A. suum* QFR. Crystals of *A. suum* QFR obtained (*a*) by the hanging-drop vapour-diffusion method using C12E8 as the main detergent and C12M as the additive detergent, (*b*) using a 3:2 weight ratio of C12E8 and C12M and (*c*) after detergent exchange to the 3:2 C12E8:C12M mixture by microdialysis.

Table 1
Statistics of data collection and processing.

Values in parentheses are for the highest resolution shell.

	A. suum QFR	*A. suum* QFR with flutolanil
X-ray source	BL44XU (SPring-8)	NW12A (Photon Factory)
Wavelength (Å)	0.900	1.000
Space group	$P2_12_12_1$	$P2_12_12_1$
Unit-cell parameters		
a (Å)	123.75	124.31
b (Å)	129.08	131.63
c (Å)	221.12	222.53
Resolution range (Å)	50.0–2.8 (2.9–2.8)	50.0–3.20 (3.35–3.20)
No. of reflections	587189	207156
Unique reflections	75372	54964
Completeness (%)	89.2 (58.8)	93.9 (84.1)
R_{merge}† (%)	10.5 (36.6)	11.5 (40.0)
$I/\sigma(I)$	8.4 (3.5)	17.4 (1.6)

† $R_{merge} = \sum_{hkl}\sum_i |I_i(hkl) - \langle I(hkl)\rangle| / \sum_{hkl}\sum_i I_i(hkl)$.

of SQR from pig heart mitochondria (Sun *et al.*, 2005; PDB code 1zoy). The sequence identities between the pig and *A. suum* enzymes are 70.4, 68.3, 34.8 and 46.3% for the Fp, Ip, CybL and CybS subunits, respectively. Using X-ray diffraction data in the resolution range 15.0–2.8 Å collected from the flutolanil-free QFR crystal, a promising solution with two molecules per asymmetric unit was obtained and an *R* factor of 0.45 was achieved when the model was subsequently subjected to rigid-body refinement. Starting from the molecular-replacement solution, the structures of the flutolanil-free and flutolanil-bound forms of the *A. suum* QFR are currently being refined and electron density corresponding to bound flutolanil has been identified. The structures of the *A. suum* QFR together with those of the QFRs from *Wolinella succinogenes* (Lancaster *et al.*, 1999) and *Escherichia coli* (Iverson *et al.*, 1999) and the SQRs from *E. coli* (Yankovskaya *et al.*, 2003), pig heart mitochondria (Sun *et al.*, 2005) and avian heart mitochondria (Huang *et al.*, 2006) should help to clarify the structure–function relationships in complex II. In addition, the structure of the *A. suum* QFR complexed with flutolanil should provide information for the structure-based design of anthelminthics.

We are grateful to the staff of BL44XU at SPring-8 and the staff of NW12 and BL-5A at Photon Factory for their help with the collection of X-ray diffraction data. This work was supported in part by a grant from the Japan Aerospace Exploration Agency and by Grants-in-Aid for Scientific Research on Priority Areas from the 21st Century COE Program (F-3), for Creative Scientific Research and Targeted Proteins Research Program from the Japanese Ministry of Education, Culture, Sports, Science and Technology (180 73004, 18GS0314 and 1903610), and for Scientific Research (B) from the Japan Society for the Promotion of Science (18370042). DKI was a research fellow supported by the Japan Society for the Promotion of Science.

References

Collaborative Computational Project, Number 4 (1994). *Acta Cryst.* D**50**, 760–763.
Ernster, L. & Nordenbrand, K. (1967). *Methods Enzymol.* **10**, 86–94.
Huang, L. S., Sun, G., Cobessi, D., Wang, A. C., Shen, J. T., Tung, E. Y., Anderson, V. E. & Berry, E. A. (2006). *J. Biol. Chem.* **281**, 5965–5972.
Inaoka, D. K., Sakamoto, K., Shimizu, H., Shiba, T., Kurisu, G., Nara, T., Aoki, T., Kita, K. & Harada, S. (2008). *Biochemistry*, **47**, 10881–10891.
Ito, Y., Muraguchi, H., Seshime, Y., Oita, S. & Yanagi, S. O. (2004). *Mol. Genet. Genomics*, **272**, 328–335.
Iverson, T. M., Luna-Chaves, C., Cecchini, G. & Rees, D. C. (1999). *Science*, **284**, 1961–1966.
Iwata, F., Shinjyo, N., Amino, H., Sakamoto, K., Islam, M. K., Tsuji, N. & Kita, K. (2008). *Parasitol. Int.* **57**, 54–61.
Jancarik, J. & Kim, S.-H. (1991). *J. Appl. Cryst.* **24**, 409–411.
Kita, K. & Takamiya, S. (2002). *Adv. Parasitol.* **51**, 95–131.
Lancaster, C. R. D., Kröger, A., Auer, M. & Michel, H. (1999). *Nature (London)*, **402**, 377–385.
Matsumoto, J., Sakamoto, K., Shinjyo, N., Kido, Y., Yamamoto, N., Yagi, K., Miyoshi, H., Nonaka, N., Katakura, K., Kita, K. & Oku, Y. (2008). *Antimicrob. Agents. Chemother.* **52**, 164–170.
Matthews, B. W. (1968). *J. Mol. Biol.* **33**, 491–497.
Miyadera, H., Shiomi, K., Ui, H., Yamaguchi, Y., Masuma, R., Tomoda, H., Miyoshi, H., Osanai, A., Kita, K. & Omura, S. (2003). *Proc. Natl Acad. Sci. USA*, **100**, 473–477.
Navaza, J. (1994). *Acta Cryst.* A**50**, 157–163.
Omura, S. *et al.* (2001). *Proc. Natl Acad. Sci. USA*, **98**, 60–62.
Otwinowski, Z. & Minor, W. (1997). *Methods Enzymol.* **276**, 307–326.
Sun, F., Huo, X., Zhai, Y., Wang, A., Xu, J., Su, D., Bartlam, M. & Rao, Z. (2005). *Cell*, **121**, 1043–1057.
Takamiya, S., Furushima, R. & Oya, H. (1984). *Mol. Biochem. Parasitol.* **13**, 121–134.
Tielens, A. G. M., Rotte, C., van Hellemond, J. J. & Martin, W. (2002). *Trends Biochem. Sci.* **27**, 564–572.
Yankovskaya, V., Horsefield, R., Törnroth, S., Luna-Chaves, C., Miyoshi, H., Léger, C., Byrne, B., Cecchini, C. & Iwata, S. (2003). *Science*, **299**, 700–704.

Mitochondrion 9 (2009) 443–453

Contents lists available at ScienceDirect

Mitochondrion

journal homepage: www.elsevier.com/locate/mito

Identification of mitochondrial Complex II subunits SDH3 and SDH4 and ATP synthase subunits *a* and *b* in *Plasmodium* spp.

Tatsushi Mogi *, Kiyoshi Kita *

Department of Biomedical Chemistry, Graduate School of Medicine, The University of Tokyo, Hongo, Bunkyo-ku, Tokyo 113-0033, Japan

ARTICLE INFO

Article history:
Received 5 February 2009
Received in revised form 3 August 2009
Accepted 6 August 2009
Available online 12 August 2009

Keywords:
ATP synthase
Membrane anchor
Mitochondria
Plasmodium
Succinate dehydrogenase

ABSTRACT

While most protist mitochondrial enzymes could be identified in database, the membrane anchor subunits of Complex II and F_oF_1-ATP synthase of malaria parasites are not annotated. Based on the presence of structural fingerprints or proteomics data from other protists, here we present their candidates. In contrast to canonical subunits, *Plasmodium* Complex II anchors have two transmembrane helices and may coordinate heme *b via* Tyr in place of His. Transmembrane helix IV of ATP synthase subunit *a* lacks an essential Arg residue. Membrane anchors of *Plasmodium* Complex II and ATP synthase are divergent from orthologs and promising targets for new chemotherapeutics.

1. Introduction

Energy metabolism in the malaria parasites is quite different from that of mammalian hosts. The erythrocytic stage cells of *Plasmodium falciparum* cause mortality associated with malaria and are considered to rely on the incomplete oxidation of glucose, with the secretion of end products such as lactate and pyruvate (Sherman, 1998). Diversity in parasite metabolism and enzyme structures will facilitate the development of new antimalarials with novel targets and mechanisms against the drug-resistant strains of *Plasmodium* spp. (Hyde, 2005).

The *Plasmodium* mitochondrion of the erythrocytic stage parasites can oxidize NADH, glycerol-3-phosphate, succinate, dihydroorotate, and amino acids (Pro and Glu), but it is essentially acristate and apparently lacks oxidative phosphorylation and a functional tricarboxylic acid (TCA) cycle (Fry and Beesley, 1991; van Dooren et al., 2006). Pyruvate dehydrogenase is targeted to the apicoplast, not to the mitochondrion (Foth et al., 2005), and thus a major carbon flow from the cytoplasm to the mitochondrion of most eukaryotes is disconnected (Fig. 1). Fumarate inhibited the NADH-dependent reduction of cytochrome *c* and stimulated the oxidation of NADH, indicating an NADH–fumarate reductase pathway for the regeneration of NAD (Fry and Beesley, 1991). Recently, Painter et al. (2007) claimed for the erythrocytic stage cells of *P. falciparum* that the mitochondrial respiratory chain is required only for the regeneration of an oxidized form of ubiquinone, which serves as the electron acceptor for type 2 dihydroorotate dehydrogenase, an essential enzyme for pyrimidine biosynthesis. Thus, it is widely accepted that the majority of the erythrocytic stage parasite's ATP demand is met through glycolysis (Carlton et al., 2002).

In the insect vector stages, malaria parasites need to adapt to changes in available carbon sources from glucose in the mammalian blood to amino acids (e.g., Pro, Glu, His, and Ala (Henn et al., 1998)) in the mosquito hemolymph, which contains the disaccharide trehalose as a dominant sugar species. As amino acids are non-fermentable carbon sources, oxidative phosphorylation with the functional TCA cycle must take place in the insect stages. Proteomic profiling studies clearly demonstrated metabolic readjustments from the glycolytic pathway in the asexual stages trophozoites and schizonts to the TCA cycle in the salivary gland sporozoites (Lasonder et al., 2008). Metabolomic studies on the erythrocytic stage *P. falciparum* demonstrated that Gln was metabolized to L-malate *via* two pathways, the reductive carboxylation pathway through citrate yielding acetyl-CoA and the oxidative pathway through succinate yielding ATP and a precursor of heme biosynthesis (δ-aminolevulinic acid) (Olszewski, Rabinowitz, Llinás, personal communication) (Fig. 1). Thus, amino acids acquired from the mosquito hemolymph or the food vacuole of the erythrocytic stage parasites can be metabolized by entering the TCA cycle as 2-oxoglutarate *via* a bifurcated mechanism using

Abbreviations: FRD, fumarate reductase; SDH, succinate dehydrogenase; TCA, tricarboxylic acid; TM, transmembrane helix.

* Corresponding authors. Tel.: +81 3 5841 3526; fax: +81 3 5841 3444.
E-mail addresses: tmogi@m.u-tokyo.ac.jp (T. Mogi), kitak@m.u-tokyo.ac.jp (K. Kita).

1567-7249/$ - see front matter © 2009 Elsevier B.V. and Mitochondria Research Society. All rights reserved.
doi:10.1016/j.mito.2009.08.004

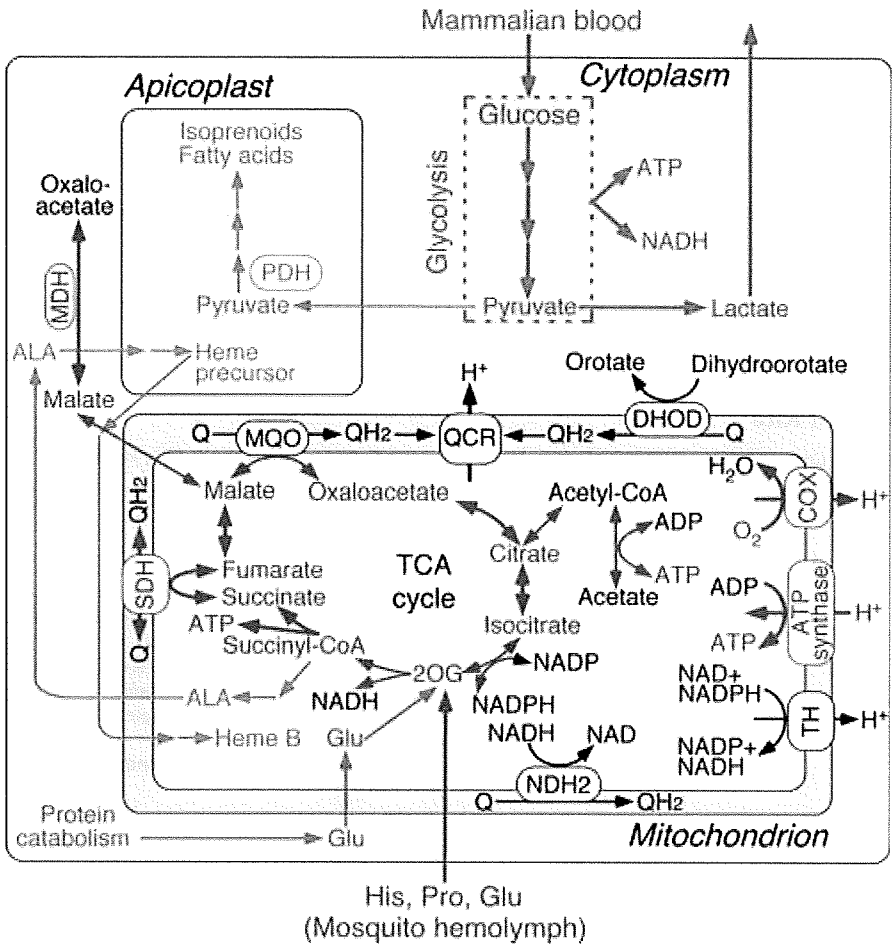

Fig. 1. Metabolic pathway in the human malaria parasite *P. falciparum*. Proton translocation machineries in the mitochondrion are F_oF_1-ATP synthase (ATPase), quinol–cytochrome *c* reductase (QCR), cytochrome *c* oxidase (COX), and NAD(P)-transhydrogenase (TH). Quinone reduction by alternative NADH dehydrogenase (NDH2), succinate dehydrogenase (SDH), malate:quinone oxidoreductase (MQO), and dihydroorotate dehydrogenase (DHOD) do not generate the proton-motive force. NAD-dependent malate dehydrogenase (MDH) and pyruvate dehydrogenase (PDH) are located in the cytoplasm and apicoplast, respectively, and do not participate in TCA cycle. Expression levels of MDH and TCA cycle enzymes (fumarate hydratase, SDH1, succinyl-CoA synthase α subunit, aconitase, and citrate synthase), and α and β subunits of ATP synthase are increased in salivary gland sporozoites while the expression levels of glycolysis pathway enzymes (hexokinase, phosphoglycerate kinase, pyruvate kinase and 6-phosphofructokinase) are increased in asexual blood-stage trophozoites and schizonts [Lasonder et al., 2008; Lasonder, Stunnenberg, personal communication]. A major carbon flow in blood-stage parasites is shown in *red* and possible carbon and energy flow in mosquito stages is shown in *blue*. Pathways absent in *B. bovis* are indicated by *green*. For the clarity, outer membranes of the mitochondrion and apicoplast are not shown. Abbreviations for metabolites are ALA (δ-aminolevulinic acid), DHAP (dihydroxyacetone phosphate), GA3P (glyceraldehyde-3-phosphate), and PEP (phosphoenolpyruvate).

the reductive and oxidative pathways. The resulting NADH and quinols are reoxidized by the respiratory chain, which indirectly drives ATP synthesis by the generation of proton-motive force.

In contrast to *P. falciparum*, the mitochondrion isolated from the erythrocytic stage rodent malaria parasite is cristate and contains more cytochromes (Fry and Beesley, 1991). Succinate respiration, ATP synthesis, and the collapse of the mitochondrial membrane potential by atovaquone (Srivastava et al., 1997), a potent inhibitor of ubiquinol–cytochrome *c* reductase (Complex III), suggest the presence of a functional oxidative phosphorylation system in the erythrocytic rodent parasite mitochondria (Uyemura et al., 2000, 2004). Transcriptome analysis of the erythrocytic human parasites, which have been isolated from infected patients, indicates that canonical mitochondrial functions exist to some extent in the human parasites (Daily et al., 2007). In *Plasmodium* spp., nuclear and mitochondrial genomes encode ubiquinol–cytochrome *c* reductase (QCR, Complex III), cytochrome *c* oxidase (COX, Complex IV), F_oF_1-ATP synthase (Complex V) and all the TCA cycle enzymes including succinate dehydrogenase (SDH, succinate–ubiquinone reductase, Complex II) (Carlton et al., 2002; Gardner et al., 2002). H^+-translocating NADH–ubiquinone reductase (NDH1, Complex I) in the mitochondrial respiratory chain is substituted by alternative NADH dehydrogenase (NDH2, a single-subunit NADH–ubiquinone reductase) (Uyemura et al., 2004; Biagini et al., 2006; Kawahara et al., 2009) (Fig. 1).

It should be noted that the membrane anchor subunits of Complex II (SDH3 (CybL) and SDH4 (CybS)) and of ATP synthase (subunits *a* (ATP6) and *b* (ATP4)) are not annotated in the current database (Carlton et al., 2002; Gardner et al., 2002), even though they are essential for transfer of chemical energy to ubiquinone and proton translocation, respectively (Fig. 2). Accordingly, the complete ATP synthase is assumed to be absent in *Plasmodium* spp. (Carlton et al., 2002; Gardner et al., 2002; Fry et al., 1990; Vaidya and Mather, 2005).

Recently, we characterized characterized Complex II of the erythrocytic stage *Plasmodium yoelii yoelii* mitochondria and found evidence for the presence of SDH3 and SDH4 (Kawahara et al., 2009). Because of the low expression of TCA cycle enzymes in

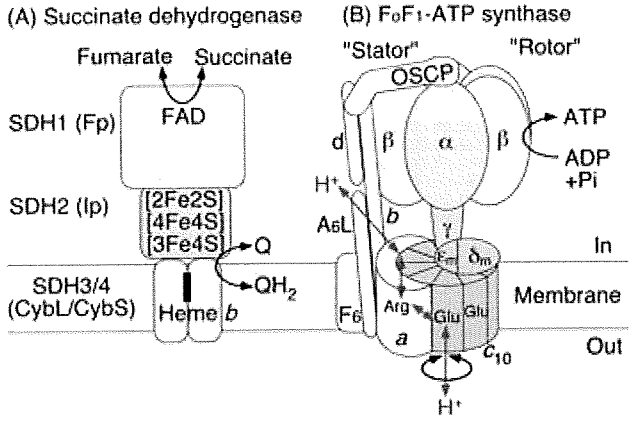

Fig. 2. Structure model for protist Complex II and ATP synthase.

the erythrocytic stage cells (Lasonder et al., 2008), sequence analysis of the anchor subunits was difficult in the *Plasmodium* mitochondria. Here we report candidates for the membrane anchor subunits of the *Plasmodium* oxidative phosphorylation enzymes. SDH3 and SDH4 of Complex II were identified by using structural fingerprints as probes while subunits *a* and *b* of ATP synthase were identified by BLAST search with proteomics data from other protists. Assignment of the membrane anchors of *Plasmodium* Complex II and ATP synthase will help our understanding of energy metabolism and the development of new antimalarials.

2. Materials and methods

2.1. Analytical methods

The presence of structural fingerprints (i.e., the heme/quinone-binding motifs) in ORFs shared by *P. falciparum* and *P. y. yoelii* genomes in the TIGR Parasite Database (http://www.tigr.org/tdb/e2k1/pya1/pya1-ortho.shtml/) was examined manually. Database searches using protein sequences were performed with the BLAST service at NCBI (http://www.ncbi.nlm.nih.gov/), GeneDB (http://www.genedb.org/), PlasmoDB (http://plasmodb.org/plasmo/), and TBestDB (http://tbestdb.bcm.umontreal.ca/). Sequences were aligned with ClustalX 2.0 (Larkin et al., 2007) and manual adjustments were made if needed. Transmembrane regions were identified with TMHMM (http://www.cbs.dtu.dk/services/TMHMM/).

3. Results and discussion

3.1. Evidence for the presence of membrane anchors of Plasmodium Complex II

Mammalian Complex II belongs to type C Complex II (Hägerhäll, 1997) and consists of four subunits and is bound to the matrix side of the inner mitochondrial membrane (Cecchini, 2003). A flavoprotein subunit (Fp, SDH1) and an iron–sulfur subunit (Ip, SDH2) form a soluble heterodimer, which then binds to a membrane anchor *b*-type cytochrome (SDH3/SDH4 heterodimer). SDH1 contains a covalently bound FAD and transfers electrons from succinate to the iron–sulfur clusters in SDH2. Electrons are then transferred to ubiquinone within a binding pocket provided by SDH2 and the SDH3/SDH4 heterodimer (Yankovskaya et al., 2003; Sun et al., 2005; Yang et al., 1998; Horsefield et al., 2006). Bacterial and mitochondrial SDH3 and SDH4 generally consist of three transmembrane helices (TM) each (I–III and IV–VI, respectively) (Yankovskaya et al., 2003; Sun et al., 2005). The quinone/heme-binding motifs, "$RPx_{16}Sx_2HR$" in TM-I and "$Hx_{10}D$" in TM-II of SDH3 and "$Hx_{10}DY$" in TM-V of SDH4 can be identified by sequence comparisons (Figs. 3 and 4). Arg31 (*Escherichia coli* Complex II numbering) in the SDH3 Sx_2HR motif and Asp82 in the SDH4 $Hx_{10}DY$ motif are in close proximity to ubiquinone and could interact with Tyr83 (Yankovskaya et al., 2003). Ser27 in the SDH3 Sx_2HR motif has been shown to be essential for quinone binding (Yang et al., 1998) and is a candidate for hydrogen bonding to the O_4 atom of ubiquinone (Horsefield et al., 2006). Tyr83 in the SDH4 $Hx_{10}DY$ motif could hydrogen bond to the O_1 atom of ubiquinone and contribute to the binding affinity (Yankovskaya et al., 2003; Horsefield et al., 2006). Examination of the *E. coli* Complex II structure (PDB 1NEK) suggests that the first arginine (Arg9 in *E. coli* SDH3) in the $RPx_{16}Sx_3R$ motif is in the vicinity of Glu186 in SDH1 and Asp106 in SDH2 and may play a structural role through a hydrogen bond network. Histidines in helices II and V (His84 and His 71 in *E. coli* SDH3 and SDH4, respectively) serve as the axial ligands for heme *b* (Yankovskaya et al., 2003; Sun et al., 2005) (Fig. 4A) but are dispensable for assembly and quinone reduction (Tran et al., 2007; Oyedotun et al., 2007).

Earlier, we have cloned and sequenced genes coding for the *P. falciparum* SDH1 and SDH2 by homology probing (Takeo et al., 2000). In contrast to these subunits, *Plasmodium* SDH3 and SDH4 appear to be highly divergent from their mitochondrial orthologs and are not annotated in the current database at NCBI, GeneDB and PlasmoDB. The *P. falciparum* Complex II previously isolated from whole cell lysates was found to be the SDH1/SDH2 heterodimer with an apparent molecular weight of 90 kDa (Suraveratum et al., 2000). The authors claimed that *Plasmodium* Complex II has a much lower K_m (3 μM) for succinate than mammalian enzymes and has the plumbagin-sensitive succinate–quinone reductase activity. However, the concentration (0.2%) of the non-ionic detergent octyl glucoside used for the isolation of *P. falciparum* Complex II was insufficient to solubilize all membrane proteins (i.e., the critical micelle concentration of octyl glucoside is 0.73%). Octyl glucoside likely dissociates the SDH1/SDH2 dimer from the membrane anchors and the aerobic isolation of the SDH1/SDH2 dimer would likely damage the iron–sulfur clusters in SDH2. Thus, the enzyme activities of such preparations need to be carefully examined. Recently, we identified *P. y. yoelii* Complex II as a 135-kDa band by native PAGE followed by activity staining (Kawahara et al., 2009). 2D-PAGE analysis of the Complex II revealed the presence of two small subunits, candidates for *Plasmodium* SDH3 and SDH4. The succinate–quinone reductase activity of *P. falciparum* and *P. y. yoelii* mitochondria (Takashima et al., 2001; Mi-Ichi et al., 2005; Kawahara et al., 2009) and succinate respiration in rodent malaria mitochondria (Uyemura et al., 2000, 2004) support the presence of membrane anchor subunits of Complex II for transferring electron to ubiquinone molecule within the inner mitochondrial membrane.

3.2. Identification of Plasmodium Complex II anchor subunits

Protist SDH3 and SDH4 are generally divergent from their orthologs, so conventional BLAST programs using bacterial and eukaryotic sequences as queries failed to identify *Plasmodium* subunits in the current genome database. Recently, we purified Complex II from the parasitic protist *Trypanosoma cruzi* and identified six each of hydrophilic and hydrophobic subunits by protein sequencing (Morales et al., 2009). Supernumerary non-catalytic

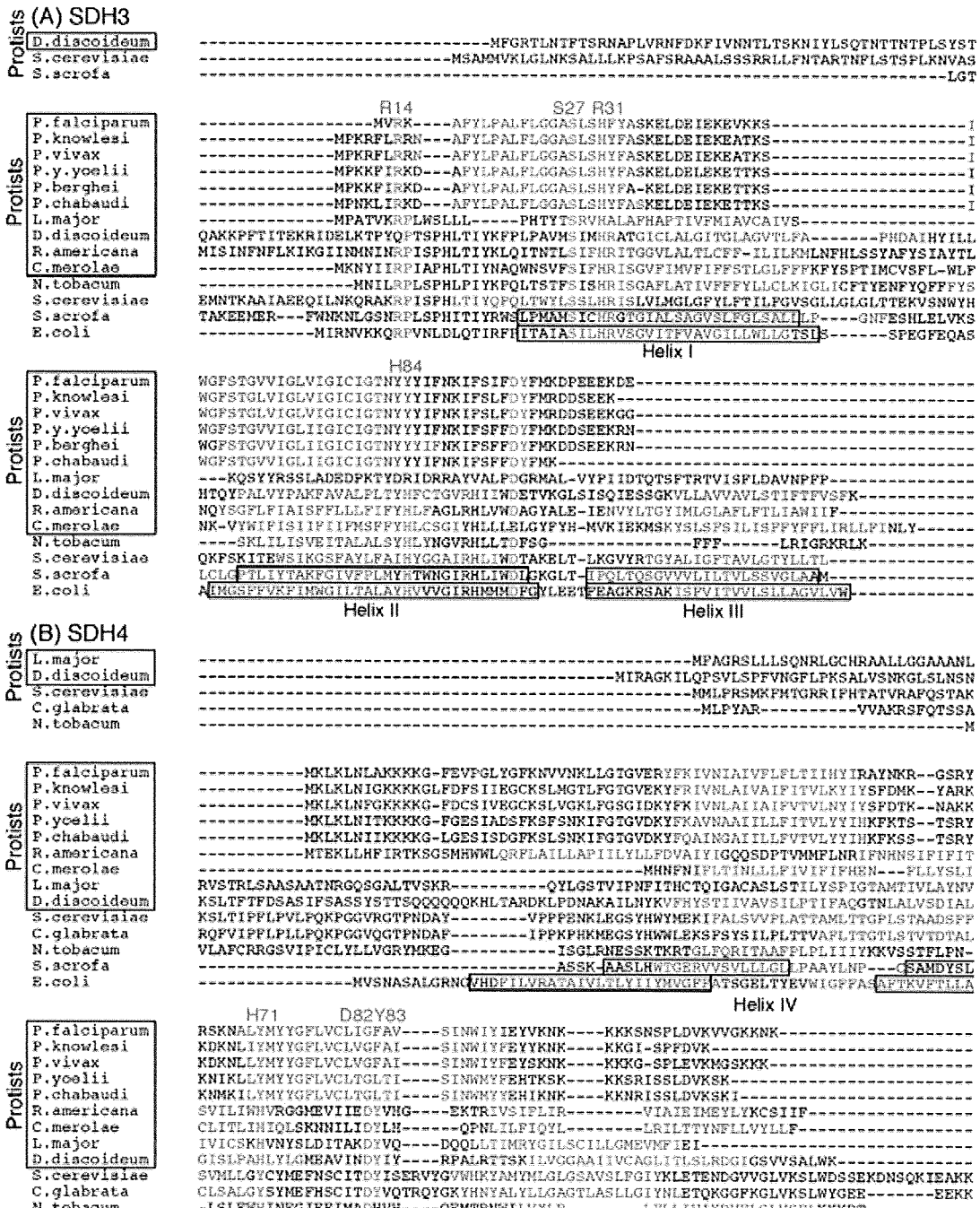

Fig. 3. Sequence alignment of SDH3 (A) and SDH4 (B) of *Plasmodium* Complex II. SDH3 and SDH4 sequences (GenBank accession Nos.) used are *P. falciparum* (XP_966100, XP_001347385), *P. knowlesi* (PKH_113810, PKH_080980), *P. vivax* (XP_001616129, XP_001614414), *P. y. yoelii* (XP_731082, XP_726783), *P. berghei* (XP_678526, not available), *P. chabaudi* (XP_742786, XP_738723), *Leishmania major* (XP_848167, XP_001685874), *Dictyostelium discoideum* (XP_643757, XP_642171), *Reclinomonas americana* (NP_044796, NP_044797), *Cyanidioschyzon merolae* (NP_059349, NP_059380), *Nicotiana tabacum* (YP_173376, YP_173457), *S. cerevisiae* S288C (NP_012781, NP_010463), *Candida glabrata* (not used, XP_446226), *Sus scrofa* (1ZOY_C, 1ZOY_D), and *E. coli* (NP_415249, NP_415250). Amino acid residues proposed for binding of ubiquinone and protoheme IX are shown in *red* and transmembrane regions predicted by TMHMM are in *blue*. Residue numbers refer to the *E. coli* SDH3 (SdhC) and SDH4 (SdhD) sequences. Transmembrane helices found in porcine Complex II (PDB 1ZOY) and *E. coli* Complex II (PDB 1NEK) are boxed.

subunits in *T. cruzi* Complex II may have evolved by complementary degeneration of dispersed duplicates (Hurles, 2004) in the Euglenozoa. Among six transmembrane subunits, we identified *T. cruzi* SDH3 and SDH4 on the basis of the presence of the quinone/heme-binding motifs, that are only conserved in these candidates (Morales et al., 2009).

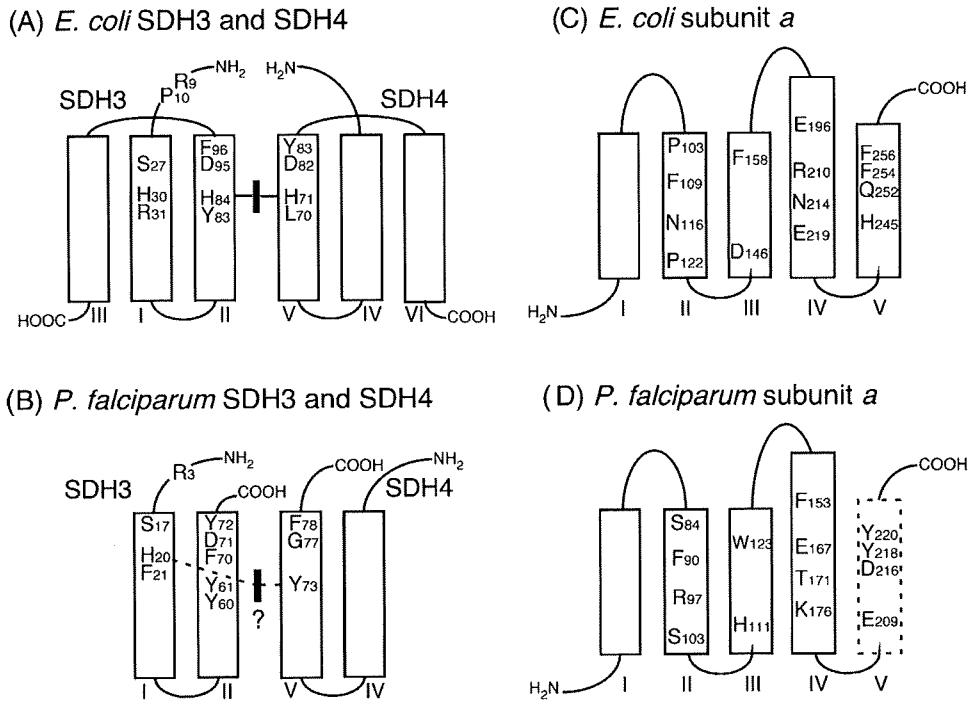

Fig. 4. Proposed structures for SDH3 and SDH4 of Complex II and subunits *a* from *E. coli* and *P. falciparum*.

Unlike *T. cruzi* mitochondria, the yield of *Plasmodium* mitochondria and the specific activity of Complex II were very low (Takashima et al., 2001; Mi-Ichi et al., 2005; Kawahara et al., 2009). Therefore, we took an alternative strategy for the identification of *Plasmodium* SDH3 and SDH4. We reexamined manually the sequences of *Plasmodium* membrane proteins for the presence of the quinone/heme-binding motifs of SDH3 and SDH4. Among 3310 ORFs[1] conserved in both *P. falciparum* and *P. y. yoelii* at the TIGR Parasite Database, 15.5% are membrane proteins with putative transmembrane segments, and 2.5% are shorter than 200 amino acid residues, as are the mitochondrial SDH3 and SDH4. From screening based on the number of TMs (1–3), spacing between TMs, conservation in *Plasmodium* spp., and the sequence motifs in transmembrane helices, we identified candidates for *P. falciparum* SDH3 (83 residues, GenBank accession No. XP_966100) and SDH4 (118 residues, XP_001347385) with two putative transmembrane helices (Figs. 3 and 4B, Table 1), which lack helices III and VI, respectively. Sequence identities of *P. falciparum* SDH3 and SDH4 against counterparts in *E. coli* and *Homo sapiens* are 15.7% and 14.3%, respectively, and 23.1% and 21.7%, respectively. An alternative candidate for PfSDH4 (XP_001349911 with one TM) contains the "YHx$_9$DY" motif but TMHMM predicts that this motif is in the *C*-terminal hydrophilic tail. Orthologs of PfSDH3 and PfSDH4 are present in human malaria parasites *Plasmodium vivax* and *Plasmodium knowlesi* and rodent malaria parasites *P. y. yoelii*, *Plasmodium berghei* and *Plasmodium chabaudi* in the current database[2]. Phylogenetic analysis of amino acid sequences showed that a clade for the membrane anchors of *Plasmodium* and Euglenozoa Complex II is an outgroup of bacterial and mitochondrial SDH3 and SDH4 (Fig. 5).

Table 1
Oxidative phosphorylation systems in *P. falciparum*.

Enzyme	Subunits	GenBank accession no.
NDH_2		XP_001352022
Succinate–quinone reductase	SDH1	XP_001347618
	SDH2	XP_001350535
	SDH3	XP_966100
	SDH4	XP_001347385
Ubiquinol:cytochrome *c* oxidoreductase	Cyt *b*	NP_059668[a]
	Rieske FeS	XP_001348547
	Cyt c_1	XP_001348771
	Hinge (QCR6)	XP_001348422
	MPP	XP_001351788, XP_001352201
Cytochrome *c*	Cyc1	XP_001348211
Cytochrome *c* oxidase	COX I	NP_059667[a] XP_001350328 (2_N)[b], XP_001348462 (2_C)[b]
	COX II	
	COX III	NP_059666[a]
	COX V	XP_001352148
	COX VI	XP_001352150
	COX VII	CAX64384
	COX VIII	XP_001351632
ATP synthase	ATP1 (α)	XP_001349675
	ATP2 (β)	XP_001350751
	ATP3 (γ)	XP_001349841
	ATP5 (OSCP, δ)	XP_001349828
	ATP16 (δ_m, ε)	XP_001348152
	ATP15 (ε_m)	XP_001349058
	ATP7 (d, p18)	XP_001348820
	ATP6 (*a*)	XP_001347344
	ATP4 (*b*)	XP_001348969
	ATP9 (*c*)	MAL7P1.340
Dihydroorotate dehydrogenase		XP_966023
NAD(P)-transhydrogenase		XP_001348682

[a] Heterodimeric COX II consist of two degenerated subunits, which retains the *N*- or *C*-terminal functional domain.

[1] Re-examination of the annotation of the *P. y. yoelii* genome on the basis of a detailed analysis of a comprehensive set of cDNA sequences and the liver stage proteome identified a further 510 genes which have orthologs in the *P. falciparum* genome (Vaughan et al., 2008). Analysis of these sequences did not yield any candidates for Complex II SDH3 and SDH4 and ATP synthase subunits *a* and *b*.

[2] The PbSDH3 sequence seems incomplete and the PbSDH4 sequence has not been identified yet at GeneDB. At NCBI, PfSDH3 was identified in *Toxoplasma gondiii* and the alternative PfSDH4 was found in other *Plasmodium* species, *T. gondii*, *Babesia bovis*, and *Theileria parva*.

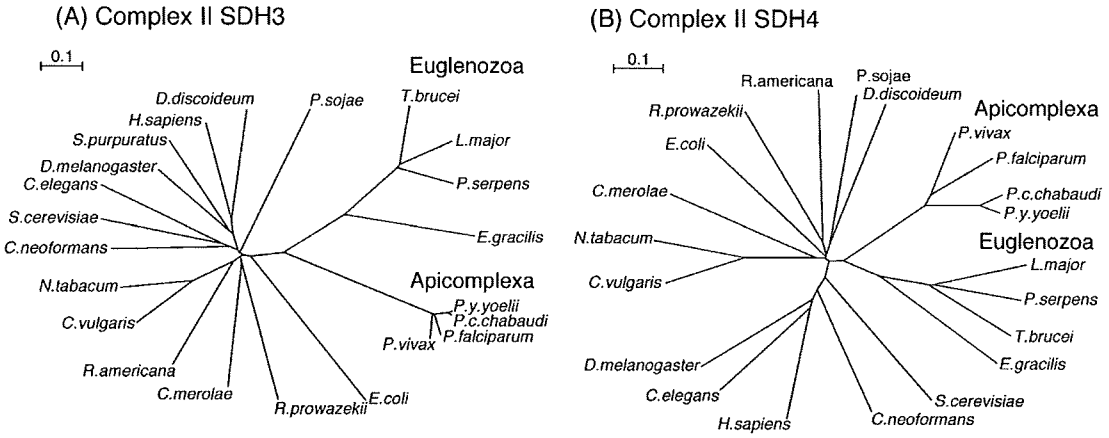

Fig. 5. Unrooted phylogenetic trees for SDH3 and SDH4 of Complex II. SDH3 and SDH4 sequences (GenBank accession Nos.) used are *H. sapiens* (NP_002992, NP_002993), *Caenorhabditis elegans* (NP_499283, NP_496369), *Cryptococcus neoformans* (XP_566692, XP_569088), *T. brucei* (XP_845531, XP_823384), *Phytomonas serpens* (CO723838, CO723900), *Euglena gracilis* (EC671331, EC610072), and *Rickettsia prowazekii* (NP_220518, NP_220519). All other sequences are described in the legend to Fig. 3.

3.3. Heme and quinone binding sites of *Plasmodium* Complex II

In *Plasmodium*, SDH3 contains an "$Rx_{13-14}Sx_2HY(F)$" motif in the *N*-terminal region of helix I and a "$YYx_{10}DY$" motif in the *C*-terminal region of helix II, in place of "$RPx_{16}Sx_2HR$" and "$YHx_{10}D$" motifs in other organisms (Figs. 3 and 4). *Plasmodium* SDH4 contains a "$Yx_{10}G$" motif in helix V in place of the canonical "$Hx_{10}DY$" motif (Figs. 3 and 4). Sequence alignments indicate that the tyrosines may substitute

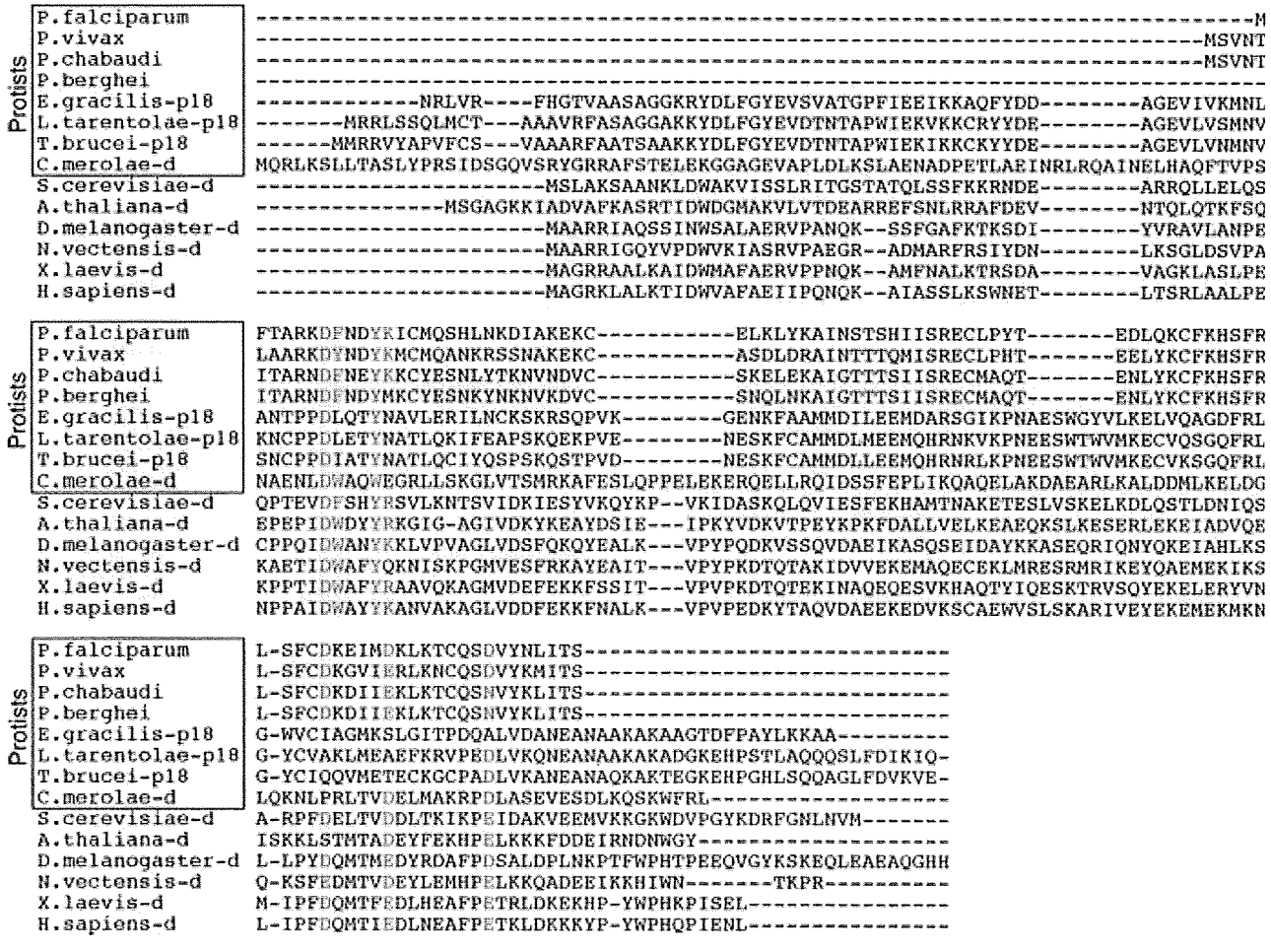

Fig. 6. Sequence alignment of subunit *d* (ATP7) of protist ATP synthase. Sequences used (GenBank accession No.) are *P. falciparum* (XP_001348820), *P. vivax* (PVX_117075), *P. c. chabaudi* (PCAS_133570), *P. berghei* (PB001416.02.0), *E. gracilis* (EC671747), *Leishmania tarentolae* (Q25423; p18), *T. brucei* (XP_844845; p18), *S. cerevisiae* (NP_012909), *Arabidopsis thaliana* (NP_190798), *Drosophila melanogaster* (NP_524402), *Nematostella vectensis* (XP_001626831), *Xenopus laevis* (NP_001084746), and *H. sapiens* (NP_006347). *C. merolae* subunit *d* sequence (CMK178C) was obtained at *Cyanidioschyzon merolae* Genome Project.

for Arg in the SDH3 "Sx_2HR" motif and histidines as heme ligands in SDH3 and SDH4 (Yankovskaya et al., 2003; Sun et al., 2005). It has been suggested that the role of a heme ligand in helix II (His84 in *E. coli* SDH3) could be replaced by a nearby histidine in the quinone-binding motif "Sx_2HR" in helix I (Maklashina et al., 2001). In SDH4 from *Saccharomyces cerevisiae* strain S288C (NP_010463) and rice (NP_001045324), the heme ligand His is substituted by Tyr and Gln, respectively. In catalase (Fita and Rossmann, 1985)

Fig. 7. Sequence alignment of subunit *b* (ATP4) of protist ATP synthase. Sequences used (GenBank accession No.) are *P. falciparum* (XP_001349752), *P. vivax* (XP_001613405), *P. berghei* (XP_680022), *P. c. chabaudi* (XP_743670), *Paramecium tetraurelia* (XP_001429993), *T. brucei* (XP_844845), *R. americana* (NP_044805), *Hemiselmis andersenii* (YP_001874763), *D. discoideum* (YP_001604088), *Phytophthora brassicae* (ES285372), *C. merolae* (NP_059355), *S. cerevisiae* (NP_015247), *Marchantia polymorpha* (NP_054459), *A. thaliana* (NP_085524), *D. melanogaster* (Q94516), *N. vectensis* (XP_001635800), *H. sapiens* (NP_001679), *Bradyrhizobium japonicum* (NP_767825), and *E. coli* (NP_418192). Domain structures shown are those proposed for *E. coli* AtpF (Dunn et al., 2000). Transmembrane helices predicted by TMHMM are indicated in *blue* and conserved residues are shown in *red*.

and other hemoproteins Tyr can coordinate the heme and the His-to-Tyr mutant of the yeast SDH3 "YHx$_{10}$D" motif retained half of the enzyme activity and heme content (Oyedotun and Lemire, 1999). In contrast to rhodoquinol–fumarate reductase (type C FRD) from parasitic nematodes (Saruta et al., 1995), menaquinol–fumarate reductase (type D FRD) from *E. coli* lacks heme *b* although membrane anchor subunits FrdC and FrdD have His and Cys, respectively, at the equivalent position of His84 and His71 of *E. coli* SdhC and SdhD, respectively (Hägerhäll, 1997; Cecchini, 2003). Depending on host environments, like *E. coli* FRD, *Plasmodium* Complex II may be able to catalyze both succinate oxidation and fumarate reduction despite *Plasmodium* mitochondria do not have low potential quinones. The presence or absence of the bound protoheme IX in *Plasmodium* Complex II and its enzymatic properties must be tested in future studies using the purified enzyme.

3.4. Membrane anchor subunits of Plasmodium ATP synthase

For a long time, it has been assumed that *Plasmodium* mitochondria cannot carry out oxidative phosphorylation (Fry and

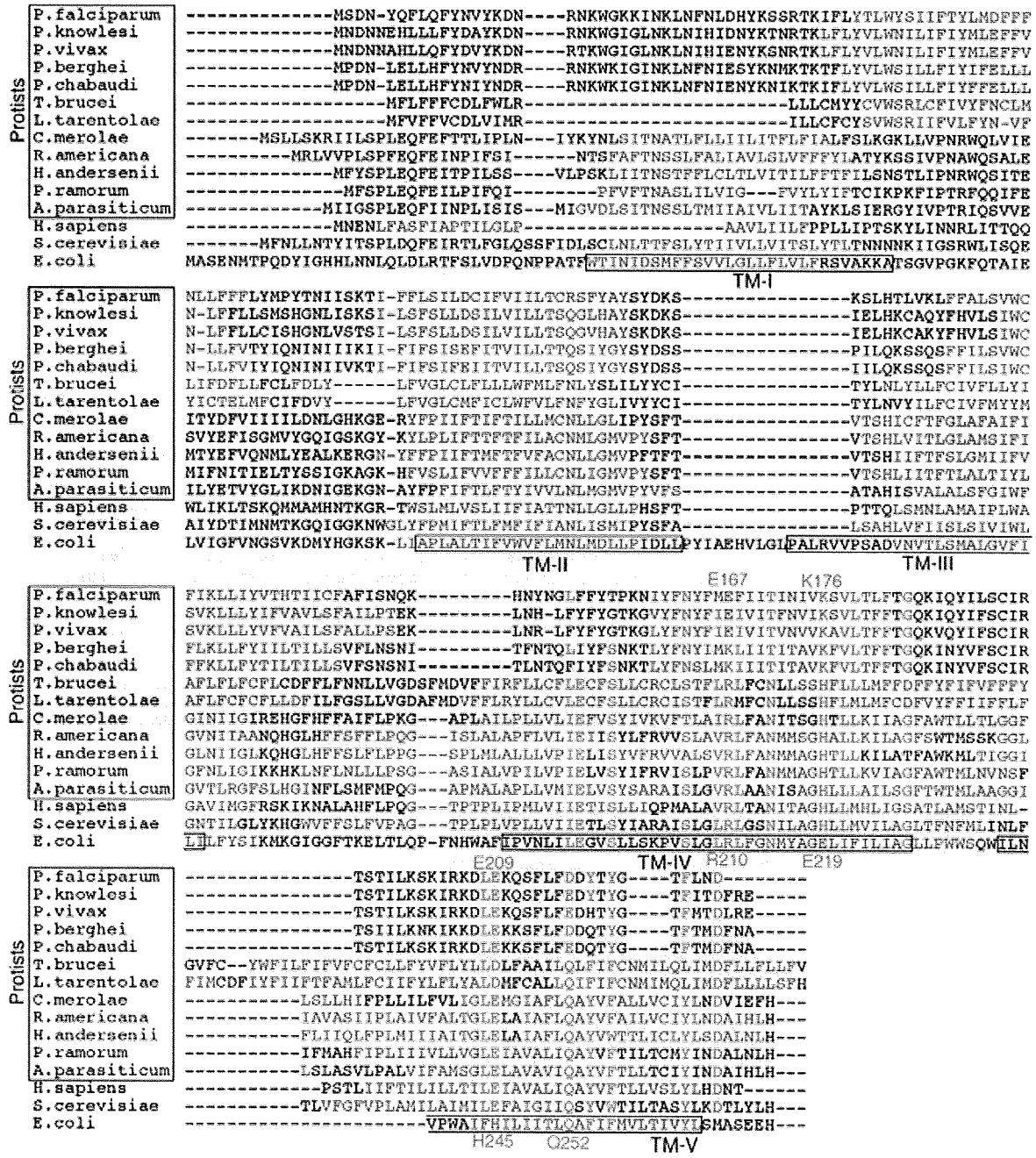

Fig. 8. Sequence alignment of subunit *a* (ATP6) of protist ATP synthase. Sequences used (GenBank accession No.) are *P. falciparum* (XP_001347344), *P. knowlesi* (CAQ39459), *P. vivax* (XP_001614365), *P. berghei* (XP_676120), *P. chabaudi* (XP_745940), *T. brucei* (AAA97428), *L. tarentolae* (AAA96695), *C. merolae* (NP_059364), *R. americana* (NP_044804), *H. andersenii* (YP_001874775), *D. discoideum* (NP_050086), *Phytophthora ramorum* (YP_001165346), *Amoebidium parasiticum* (AAN04079), *H. sapiens* (NP_536848), *S. cerevisiae* (CAA24054), and *E. coli* (NP_418194). Transmembrane helices (TM) predicted by TMHMM are indicated in *blue* and those proposed for *E. coli* AtpB (Moore et al., 2008) are boxed. Conserved amino acid residues in TM-IV and -V are shown in *red*.

Beesley, 1991) because of the apparent lack of transmembrane subunits *a* and *b* of the H^+-translocating F_oF_1-ATP synthase (Carlton et al., 2002; Gardner et al., 2002). However, oxidative phosphorylation in rodent malaria mitochondria (Uyemura et al., 2000, 2004) supports the presence of subunits *a* an *b* of the F_o subcomplex, which serve as the stator in the rotary mechanism (Noji et al., 1997; Fillingame et al., 2000) (Fig. 2), in *Plasmodium* ATP synthase.

Subunits *a* and *b* of protist ATP synthase are also highly divergent from bacterial and eukaryotic counterparts and are frequently not anotated in the database (Seeber et al., 2008). In mitochondrial genomes of land plants and certain protists, ORFs *ymf19* (*orfB*) and *ymf39* are conserved. Based on the sequence similarity and of mass spectrometric analysis, *Ymf19/OrfB* was assigned as subunit ATP8 (A6L) of the sunflower ATP synthase (Sabar et al., 2003). By protein sequencing and mass spectrometric analysis, Ymf39 was assigned as subunit *b* (ATP4 in mitochondria, AtpF in bacteria) in the jakobid *Seculamonas ecuadoriensis* (Burger et al., 2003), and the kinetoplastids *Crithidia fasciculata* (Speijer et al., 1997) and *Leishmania tarentolae* (Nelson et al., 2004). Based on peptide sequences of the *C. fasciculate* ATP synthase subunits, Allen et al. (2004) identified seven subunits of *Trypanosoma brucei* ATP synthase. By using these protist sequences as queries, we identified candidates for 10 subunits of *Plasmodium* ATP synthase with the current database (Table 1). In the mitochondrial ATP synthase, subunits *b* and ε of bacterial enzymes are split to subunits *b* and *d* and subunits δ_m and ε_m, respectively. We noticed that ATP16 (ε, δ_m) was mislabeled as ATP15 (ε_m) in *T. brucei* ATP synthase (Allen et al., 2004). Trypanosomatid p18 has been assigned as subunit *b* in previous studies (Nelson et al., 2004; Zíková et al., 2009). It is a hydrophilic nuclear gene product and our sequence analysis indicates that trypanosomatid and euglenid p18s are more closely related to subunit *d* (ATP7) (Devenish et al., 2000) (Fig. 6). As discussed by Burger et al. (2003), subunit *b* is rather featureless except for the locations of its transmembrane helices in the *N*-terminal region (Dunn et al., 2000) and there is no strictly conserved residue throughout species (Fig. 7).

Since the *C. fasciculate* band 3 homolog has four putative transmembrane helices, we tentatively assigned band 3 as subunit *a* (ATP6, AtpB) among four unassigned subunits of *T. brucei* ATP synthase (Allen et al., 2004). Using the *T. brucei* sequence as a query, we identified *Plasmodium* subunit *a* (Fig. 8). The sequence identities of *P. falciparum* subunit *a* with the *E. coli* AtpB (Fig. 4C) and *H. sapiens* ATP6 are 12.9% and 18.8%, respectively. TM-I of *Plasmodium* and *Trypanosoma* spp. showed a high sequence similarity and TM-IV and TM-V are conserved throughout species. Arg210 in transmembrane helix IV (*E. coli* AtpB numbering), which is essential for the proton translocation through the F_o subcomplex (Valiyaveetil and Fillingame, 1977; Fillingame et al., 2000; Moore et al., 2008), is substituted by Glu and Lys in human and rodent malaria parasites, respectively (Figs. 4D and 8). In *E. coli*, second site suppressor mutations of Arg210Gln in TM-IV have been identified as Gln252Arg and Gln252Lys in TM-V (Hatch et al., 1995; Ishmukhametov et al., 2008), indicating close proximity of these conserved residues. Notably, a pair of residues at positions 219 and 245 of *E. coli* subunit *a* are interchanged in mitochondria and the *E. coli* double mutant Glu219His/His245Glu was a slightly functional (Cain and Simoni, 1988). In the malaria parasites, Gln252 is replaced by Asp or Glu and Glu219 and His245 by Lys and Glu, respectively. Despite a lack of Arg210, a set of amino acid substitutions would make the *Plasmodium* subunit *a* functional.

In conclusion, here we identified candidates for six F_1 subunits [α, β, γ, δ (ATP5, OSCP), δ_m, and ε_m] and four F_o subunits (*a–d*) in *Plasmodium* spp (Table 1). Thus, the *Plasmodium* ATP synthase contains all eight subunits of the *E. coli* ATP synthase ($\alpha_3\beta_3\gamma_1\delta_1\varepsilon$-(=$\delta_m$ *plus* ε_m)$_1a_1b$(=*b plus d*)$_1c_{10?}$) and could carry out a rotary mechanism for ATP synthesis (Noji et al., 1997; Fillingame et al., 2000). Phylogenetic analysis showed that, in contrast to soluble catalytic subunit β (not shown), all three membrane anchor subunits, *a*, *b* (Fig. 9) and *c* (not shown), of *Plasmodium* and *Trypanosoma* spp. are divergent from their mitochondrial orthologs. Diversity in membrane anchors of parasitic protist mitochondrial ATP synthase suggests the plasticity in their structures even though they are essential for oxidative phosphorylation. Such variations may modulate or attenuate the function in host environments.

4. Conclusion and perspectives

We identified candidates for the membrane anchors of *Plasmodium* Complex II based on the presence of the structural fingerprints and showed sequence divergence from the eukaryotic orthologs. ATPase subunits *a* and *b* of *Plasmodium* were identified based on proteomics data of other protists, and again we found high sequence divergence in the membrane anchors. Our studies

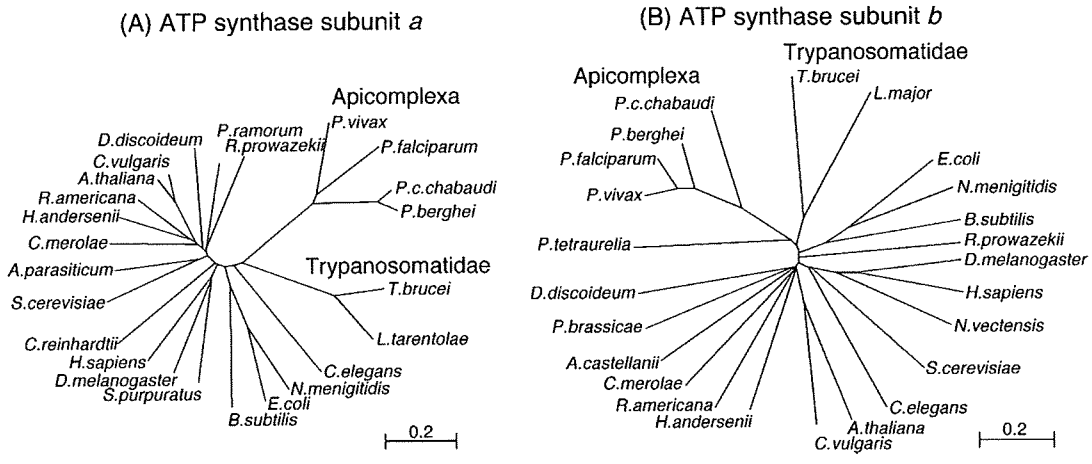

Fig. 9. Unrooted phylogenetic trees for subunit *a* (A) and *b* (B) of F-type ATP synthase. Subunits *a* and *b* sequences (GenBank accession Nos.) used are *D. melanogaster* (NP_008281, Q94516), *C. elegans* (NP_006956, NP_497938), *Strongylocentrotus purpuratus* (NP_006971, not available), *A. thaliana* (NP_085569, NP_085524), *Chara vulgaris* (NP_943689, NP_943702), *Chlamydomonas reinhardtii* (XP_001689492, not available), *L. major* (not available, XP_001686628), *Acanthamoeba castellanii* (not available, NP_042558), *R. prowazekii* (NP_220417, NP_220414), *Neisseria meningiditis* (NP_274934, NP_274932), and *Bacillus subtilis* (NP_391568, NP_391566). All other sequences were described in the legends to Figs. 7 and 8. The mitochondrial genomes encode eukaryotic subunits *a* except *C. reinhardtii* and *Plasmodium* spp. and subunit *b* of plants and some protists (*D. discoideum*, *C. merolae*, *R. americana*, and *H. andersenii*).

suggest that *Plasmodium* mitochondria possess all catalytic subunits for Complex II and ATP synthase (Table 1) and are fully capable of oxidative phosphorylation. Our approach is applicable to other membrane proteins although it is rather low throughput. Our assignments should help in understanding parasite energy metabolism.

Recently, diarylquinoline, a new tuberculosis-specific agent, has been shown to bind subunit *c* of ATP synthase (Andries et al., 2005). *Plasmodium* Complex II and ATP synthase could be pathogen-specific targets for new antimalarial agents, because of sequence divergence in membrane anchor subunits. In addition, alternative respiratory enzymes like NDH2 and malate:quinone oxidoreductase (MQO) are absent in mammalian mitochondria and are also promising targets. Since inhibitors for NDH2 are rare and mostly nonspecific (Kerscher, 2000), we screened natural antibiotics and identified gramicidin S and scopafungin as new inhibitors (Mogi et al., 2009). (Saleh et al., 2007) found that 1-hydroxy-2-dodecyl-4(1*H*)quinolone (HDQ), a potent inhibitor for yeast NDH2 (Eschemann et al., 2005), can act as an antimalarial. Even though our compounds were less effective on the *Plasmodium* enzyme than on bacterial enzymes, they may still serve as antimalarials. Such continuing efforts on the screening of natural and synthetic compounds could identify novel and potent drugs against malaria.

Acknowledgements

This study was supported by a grant-in-aid for scientific research (20570124 to TM) and Creative Scientific Research (18GS0314 to KK) from the Japan Society for the Promotion of Science, and a grant-in-aid for scientific research on Priority Areas (18073004 to KK) from the Ministry of Education, Culture, Sports, Science and Technology, Japan. We would like to thank Dr. B. Lemire (University of Alberta), Dr. G. Burger (University of Montreal), and Dr. S. Sato (National Institute for Medical Research, UK) for critical reading of the manuscript, Dr. M. Llinás (Princeton University), Dr. L. Lasonder, and Dr. H.E. Stunnenberg (Radboud University Nijmegen) for the use of their unpublished results.

References

Allen, J.W.A., Ginger, M.L., Ferguson, S.J., 2004. Maturation of the unusual single-cysteine (XXXCH) mitochondrial *c*-type cytochromes found in trypanosomatids must occur through a novel biogenesis pathway. Biochem. J. 383, 537–542.

Andries, K., Verhasselt, P., Guillemont, J., Göhlmann, H.W.H., Neefs, J.M., Winkler, H., Gestel, J.V., Timmerman, P., Zhu, M., Lee, E., Williams, P., de Chaffoy, D., Huitric, E., Hoffner, S., Cambau, E., Truffot-Pernot, C., Lounis, N., Jarlier, V., 2005. A diarylquinoline drug active on the ATP synthase of *Mycobacterium tuberculosis*. Science 307, 223–227.

Biagini, G.A., Viriyavejakul, P., O'Neill, P.M., Bray, P.G., Ward, S.A., 2006. Functional characterization and target validation of alternative Complex I of *Plasmodium falciparum* mitochondria. Antimicrob. Agents Chemother. 50, 1841–1851.

Burger, G., Lang, B.F., Braun, H.-P., Marx, S., 2003. The enigmatic mitochondrial ORF *ymf39* codes for ATP synthase chain *b*. Nucleic Acids Res. 31, 2353–2360.

Cain, B.D., Simoni, R.D., 1988. Interaction between Glu-219 and His-245 within the *a* subunit of F_1F_0-ATPase in *Escherichia coli*. J. Biol. Chem. 263, 6606–6612.

Carlton, J.M., Angiuoli, S.V., Suh, B.B., Kooij, T.W., Pertea, M., Silva, J.C., Ermolaeva, M.D., Allen, J.E., Selengut, J.D., Koo, H.L., Peterson, J.D., Pop, M., Kosack, D.S., Shumway, M.F., Bidwell, S.L., Shallom, S.J., van Aken, S.E., Riedmuller, S.B., Feldblyum, T.V., Cho, J.K., Quackenbush, J., Sedegah, M., Shoaibi, A., Cummings, L.M., Florensk, L., Yatesk, J.R., Raine, J.D., Sinden, R.E., Harris, M.A., Cunningham, D.A., Preiser, P.R., Bergman, L.W., Vaidya, A.B., van Lin, L.H., Janse, C.J., Waters, A.P., Smith, H.O., White, O.R., Salzberg, S.L., Venter, J.C., Fraser, C.M., Hoffman, S.L., Gardner, M.J., Carucci, D.J., 2002. Genome sequence and comparative analysis of the model rodent malaria parasite *Plasmodium yoelii yoelii*. Nature 419, 512–519.

Cecchini, G., 2003. Function and structure of Complex II of the respiratory chain. Annu. Rev. Biochem. 72, 77–109.

Daily, J.P., Scanfeld, D., Pochet, N., Roch, K.L., Plouffe, D., Kamel, M., Sarr, O., Mboup, S., Ndir, O., Wypij, D., Lavasseur, K., Thomas, E., Tamayo, P., Dong, C., Zhou, Y., Lander, E.S., Ndiaye, D., Wirth, D., Winzeler, E.A., Mesirov, J.P., Regev, A., 2007. Distinct physiological states of *Plasmodium falciparum* in malaria-infected patients. Nature 450, 1091–1095.

Devenish, R.J., Prescott, M., Roucou, X., Nagley, P., 2000. Insights into ATP synthase assembly and function through the molecular genetic manipulation of subunits of the yeast mitochondrial enzyme complex. Biochim. Biophys. Acta 1458, 428–442.

Dunn, S.D., McLachlin, D.T., Revington, M., 2000. The second stalk of *Escherichia coli* ATP synthase. Biochim. Biophys. Acta 1468, 356–363.

Eschemann, A., Galkin, A., Oettmeier, W., Brandt, U., Kerscher, S., 2005. HDQ (1-hydroxy-2-dodecyl-4(1*H*)quinolone), a high affinity inhibitor for mitochondrial alternative NADH dehydrogenase: evidence for a ping-pong mechanism. J. Biol. Chem. 280, 3138–3142.

Fillingame, R.H., Jiang, W., Dimitriev, O.Y., 2000. Coupling of H^+ transport to rotary catalysis in F-type ATP synthases: structure and organization of the transmembrane rotary motor. J. Exp. Biol. 203, 9–17.

Fita, I., Rossmann, M.G., 1985. The active center of catalase. J. Mol. Biol. 185, 21–37.

Foth, B.J., Stimmler, L.M., Handman, E., Crabb, B.S., Hodder, A.N., McFadden, G.I., 2005. The malaria parasite *Plasmodium falciparum* has only one pyruvate dehydrogenase complex, which is located in the apicoplast. Mol. Microbiol. 55, 39–53.

Fry, M., Webb, E., Pudney, M., 1990. Effect of mitochondrial inhibitors on adenosine triphosphate levels in *Plasmodium falciparum*. Comp. Biochem. Physiol. B 96, 775–782.

Fry, M., Beesley, J.E., 1991. Mitochondria of mammalian *Plasmodium* spp. Parasitology 102, 17–26.

Gardner, M.J., Hall, N., Fung, E., White, O., Berriman, M., Hyman, R.W., Carlton, J.M., Pain, A., Nelson, K.E., Bowman, S., Paulsen, I.T., James, K., Eisen, J.A., Rutherford, K., Salzberg, S.L., Craig, A., Kyes, S., Chan, M.S., Nene, V., Shallom, S.J., Suh, B., Peterson, J., Angiuoli, S., Pertea, M., Allen, J., Selengut, J., Haft, D., Mather, M.W., Vaidya, A.B., Martin, D.M., Fairlamb, A.H., Fraunholz, M.J., Roos, D.S., Ralph, S.A., McFadden, G.I., Cummings, L.M., Subramanian, G.M., Mungall, C., Venter, J.C., Carucci, D.J., Hoffman, S.L., Newbold, C., Davis, R.W., Fraser, C.M., Barrell, B., 2002. Genome sequence of the human malaria parasite *Plasmodium falciparum*. Nature 419, 498–511.

Hägerhäll, C., 1997. Succinate: quinone oxidoreductases. Variations on a conserved theme. Biochim. Biophys. Acta 1320, 107–141.

Hatch, L.P., Cox, G.B., Howitt, S.M., 1995. The essential arginine residue at position 210 in the *a* subunit of the *Escherichia coli* ATP synthase can be transferred to position 252 with partial retention of activity. J. Biol. Chem. 270, 29407–29412.

Henn, M.W., Schopf, R., Maier, W.A., Seitz, H.M., 1998. The amino acid composition of *Anopheles stephensi* (Diptera: Culicidae) infected with *Nosema algerae* (Microsporida: Nosematidae). J. Invertebr. Pathol. 71, 42–47.

Horsefield, R., Yankovskaya, V., Sexton, G., Whittingham, W., Shiomi, K., Ōmura, S., Byrne, B., Cecchini, G., Iwata, S., 2006. Structural and computational analysis of the quinone-binding site of Complex II (succinate–ubiquinone oxidoreductase). A mechanism of electron transfer and proton conduction during ubiquinone reeuction. J. Biol. Chem. 281, 7309–7316.

Hurles, M., 2004. Gene duplication: the genomic trade in spare parts. PLoS Biol. 2, 0900–0904.

Hyde, J.E., 2005. Drug-resistant malaria. Trends Parasitol. 21, 494–498.

Ishmukhametov, R.R., Pond, J.B., Al-Huqail, A., Galkin, M.A., Vik, S.B., 2008. ATP synthesis without R210 of subunit *a* in the *Escherichia coli* ATP synthase. Biochim. Biophys. Acta 1777, 32–38.

Kawahara, K., Mogi, T., Tanaka, T.Q., Hata, M., Miyoshi, H., Kita, K., 2009. Mitochondrial dehydrogenases in the aerobic respiratory chain of the rodent malaria parasite *Plasmodium yoelii yoelii*. J. Biochem. 145, 229–237.

Kerscher, S.J., 2000. Diversity and origin of alternative NADH:ubiquinone oxidoreductase. Biochim. Biophys. Acta 1459, 274–283.

Larkin, M.A., Blackshields, G., Brown, N.P., Chenna, R., McGettigan, P.A., McWilliam, H., Valentin, F., Wallace, I.M., Wilm, A., Lopez, R., Thompson, J.D., Gibson, T.J., Higgins, D.G., 2007. ClustalW2 and ClustalX version 2. Bioinformatics 23, 2947–2948.

Lasonder, E., Janse, C.J., van Gemert, G., Mair, G.R., Vermunt, A.M.W., Douradinha, B.G., van Noort, V., Huynen, M.A., Luty, A.J.F., Kroeze, H., Khan, S.M., Sauerwein, R.W., Waters, A.P., Mann, M., Stunnenberg, H.G., 2008. Proteomic profiling of *Plasmodium* sporozoite maturation identifies new proteins essential for parasite development and infectivity. PLoS Pathogens 4, e1000195.

Maklashina, E., Rothery, R.A., Weiner, J.H., Cecchini, G., 2001. Retention of heme in axial ligand mutants of succinate–ubiquinone oxidoreductase (Complex II) from *Escherichia coli*. J. Biol. Chem. 276, 18968–18976.

Mi-Ichi, F., Miyadera, H., Kobayashi, T., Takamiya, S., Waki, S., Iwata, S., Shibata, S., Kita, K., 2005. Parasite mitochondria as a target of chemotherapy: inhibitory effect of licochalcone A on the *Plasmodium falciparum* respiratory chain. Ann. NY. Acad. Sci. 1056, 46–54.

Mogi, T., Matsushita, K., Miyoshi, H., Ui, H., Shiomi, K., Ōmura, S., Kita, K., 2009. Identification of new inhibitors for alternative NADH dehydrogenase (NDH-II). FEMS Microbiol. Lett. 291, 157–161.

Moore, K.J., Angevine, C.M., Vincent, O.D., Schwem, B.E., Fillingame, R.H., 2008. The cytoplasmic loops of subunit a of *Escherichia coli* ATP synthase may participate in the proton translocation mechanism. J. Biol. Chem. 283, 13044–13052.

Morales, J., Mogi, T., Mineki, S., Takashima, E., Mineki, R., Hirawake, H., Sakamoto, K., Ōmura, S., Kita, K., 2009. Novel mitochondrial Complex II isolated from *Trypanosoma cruzi* is composed of twelve peptides including a heterodimeric Ip subunit. J. Biol. Chem. 284, 7255–7263.

Nelson, R.E., Aphasizheva, I., Falick, A.M., Nebohacova, M., Simpson, L., 2004. The I-complex in *Leishmania tarentolae* is an uniquely-structured F_1-ATPase. Mol. Biochem. Parasitol. 135, 221–224.

Noji, H., Yasuda, R., Yoshida, M., Kinosita, K., 1997. Direct observation of the rotation of F_1-ATPase. Nature 386, 299–302.

Oyedotun, K.S., Lemire, B.D., 1999. The *Saccharomyces cerevisiae* succinate–ubiquinone oxidoreductase. Identification of Sdh3p amino acid residues involved in ubiquinone binding. J. Biol. Chem. 274, 23956–23962.

Oyedotun, K.S., Sit, C.S., Lemire, B.D., 2007. The *Saccharomyces cerevisiae* succinate dehydrogenase does not require heme for ubiquinone reduction. Biochim. Biophys. Acta 1767, 1436–1445.

Painter, H.J., Morrisey, J.M., Mather, M.W., Vaidya, A.B., 2007. Specific role of mitochondrial electron transport in blood-stage *Plasmodium falciparum*. Nature 446, 88–91.

Sabar, M., Gagliardi, D., Balk, J., Leaver, C., 2003. ORFB is a subunit of F_1F_o-ATP synthase: insight into the basis of cytoplasmic male sterility in sunflower. EMBO Rep. 4, 381–386.

Saleh, A., Friesen, J., Baumeister, S., Gross, G., Bohne, W., 2007. Growth inhibition of *Toxoplasma gondii* and *Plasmodium falciparum* by nanomolar concentrations of 1-hydroxy-2-dodecyl-4(1*H*)quinolone, a high-affinity inhibitor of alternative (type II) NADH dehydrogenases. Antimicrob. Agents Chemother. 51, 1217–1222.

Saruta, F., Kuramochi, T., Nakamura, K., Takamiya, S., Yu, Y., Aoki, T., Sekimizu, K., Kojima, S., Kita, K., 1995. Stage-specific isoforms of complex II (succinate–ubiquinone oxidoreductase) in mitochondria from the parasitic nematode, *Ascaris suum*. J. Biol. Chem. 270, 928–932.

Seeber, F., Limenitakis, J., Soldati-Favre, D., 2008. Apicomplexan mitochondrial metabolism: a story of gains, losses and retentions. Trends Parasitol. 24, 468–478.

Sherman, I.W., 1998. Carbohydrate metabolism of asexual stages. In: Sherman, I.W. (Ed.), Malaria, Parasite Biology, Pathogenesis and Protection. ASM Press, Washington, DC, pp. 135–143.

Speijer, D., Breek, C.K., Muijsers, A.O., Hartog, A.F., Berden, J.A., Albracht, S.P., Samyn, B., van Beeumen, J., Benne, R., 1997. Characterization of the respiratory chain from cultured *Crithidia fasciculate*. Mol. Biochem. Parasitol. 85, 171–186.

Srivastava, I.K., Rottenberg, H., Vaidya, A.B., 1997. Atovaquone, a broad spectrum antiparasitic drug, collapses mitochondrial membrane potential in malarial parasite. J. Biol. Chem. 272, 3961–3966.

Sun, F., Huo, X., Zhai, Y., Wang, A., Xu, J., Su, D., Bartlam, M., Rao, Z., 2005. Crystal structure of mitochondrial respiratory membrane protein complex II. Cell 121, 1043–1057.

Suraveratum, N., Krungkrai, S.R., Leangaramgul, P., Prapunwattana, P., Krungkrai, J., 2000. Purification and characterization of *Plasmodium falciparum* succinate dehydrogenase. Mol. Biochem. Parasitol. 105, 215–222.

Takashima, E., Takamiya, S., Takeo, S., Mi-ichia, F., Amino, H., Kita, K., 2001. Isolation of mitochondria from *Plasmodium falciparum* showing dihydroorotate dependent respiration. Parasitol. Int. 50, 273–278.

Takeo, S., Kokaze, A., Ng, C.S., Mizuchi, D., Watanabe, J.I., Tanabe, K., Kojima, S., Kita, K., 2000. Succinate dehydrogenase in *Plasmodium falciparum* mitochondria: molecular characterization of the *SDHA* and *SDHB* genes for the catalytic subunits, the flavoprotein (Fp) and iron–sulfur (Ip) subunits. Mol. Biochem. Parasitol. 107, 191–205.

Tran, Q.M., Rothery, R.A., Maklashina, E., Cecchini, G., Weiner, J.H., 2007. *Escherichia coli* succinate dehydrogenase variant lacking the heme *b*. Proc. Natl. Acad. Sci. USA 104, 18007–18012.

Uyemura, S.A., Luo, S., Moreno, S.N.J., Docampo, R., 2000. Oxidative phosphorylation, Ca^{2+} transport, and fatty acid-induced uncoupling in malaria parasites mitochondria. J. Biol. Chem. 275, 9709–9715.

Uyemura, S.A., Luo, S., Vieira, M., Moreno, S.N., Docampo, R., 2004. Oxidative phosphorylation and rotenone-insensitive malate- and NADH-quinone oxidoreductases in *Plasmodium yoelii yoelii* mitochondria *in situ*. J. Biol. Chem. 279, 385–393.

Vaidya, A.B., Mather, M.W.A., 2005. Post-genomic view of the mitochondrion in malaria parasites. Curr. Top. Microbiol. Immunol. 295, 233–250.

Valiyaveetil, F.I., Fillingame, R.H., 1977. On the role of Arg-210 and Glu-219 of subunit *a* in proton translocation by the *Escherichia coli* F_OF_1-ATP synthase. J. Biol. Chem. 272, 32635–32641.

van Dooren, G.G., Stimmler, L.M., McFadden, G.I., 2006. Metabolic maps and functions of the *Plasmodium* mitochondrion. FEMS Microbiol. Rev. 30, 596–630.

Vaughan, A., Chiu, S., Ramasamy, G., Li, L., Gardner, M.J., Tarun, A.S., Kappe, S.H.I., Peng, X., 2008. Assessment and improvement of the *Plasmodium yoelii yoelii* genome annotation through comparative analysis. ISMB 24, i383–i389.

Yang, X., Yu, L., He, D., Yu, C.A., 1998. The quinone-binding site in succinate–ubiquinone reductase from *Escherichia coli*. Quinone-binding domain and amino acid residues involved in quinone binding. J. Biol. Chem. 273, 31916–31923.

Yankovskaya, V., Horsefield, R., Tornroth, S., Luna-Chavez, C., Miyoshi, H., Leger, C., Byrne, B., Cecchini, G., Iwata, S., 2003. Architecture of succinate dehydrogenase and reactive oxygen species generation. Science 299, 700–704.

Zíková, A., Schnaufer, A., Dalley, R.A., Panigrahi, A.K., Stuart, K.D., 2009. The F_OF_1-ATP synthase complex contains novel subunits and is essential for procyclic *Trypanosoma brucei*. PLoS Pathogens 5, e1000436.

Acta Crystallographica Section F
Structural Biology and Crystallization Communications
ISSN 1744-3091
Editors: H. M. Einspahr and M. S. Weiss

Crystallization and preliminary X-ray analysis of aspartate transcarbamoylase from the parasitic protist *Trypanosoma cruzi*

Kazuaki Matoba, Takeshi Nara, Takashi Aoki, Teruki Honma, Akiko Tanaka, Masayuki Inoue, Shigeru Matsuoka, Daniel Ken Inaoka, Kiyoshi Kita and Shigeharu Harada

Acta Cryst. (2009). F**65**, 933–936